

14

New Energy Times Archive



UNIVERSITY OF MISSOURI-COLUMBIA

August 22, 1989

College of Engineering

Nuclear Engineering

Electrical Engr. Bldg.
Columbia, Missouri 65211
Telephone (314) 882-3550

Dr. William Woodard
U.S. Department of Energy
ER-6, 3F-061
Office of Energy Research
1000 Independence Ave., SW
Washington, DC 20077-9381

Dear Dr. Woodard,

My cold fusion work does not use electrolytic cells. Instead, I have chosen to develop a method of loading palladium (and other materials) with deuterium using a plasma. In addition, I have tried to reproduce the results of Scaramuzzi at the Centro Energia Reserchei Frascati and Menlove at Los Alamos National Lab using high and subatmospheric deuterium pressures and temperature to load Ti and Pd.

I have used an RGA to look at the mass spectra of gases in these experiments. Masses of 1, 2, 3, 4, 5 and 6 amu were observed but can be explained by the presence of H^+ , D^+ , DH^+ , D_2^+ , D_2H^+ and D_3^+ respectively. I am planning to accumulate gas samples and have them analyzed for tritium decay in the near future.

I have observed very low level neutron emission from the plasma loaded palladium experiments indicative of a fusion rate of about 1×10^{-23} fusion reactions per D_2 per second. Additionally, prompt gamma emission at 8.11 MeV was observed in these experiments. I presently do not understand the 8.11 MeV gamma emission. With regard to the pressure and temperature loading of palladium, I have observed bursts of neutrons. I have used two helium-3 detector redundancy for these experiments. My best results have come from Pd powder.

If you have any further questions, please feel free to contact me.

Sincerely,

Mark A. Prelas
Professor and Ketchum Research Professor

Enclosure

c: Jacob Bigeleisen

MAP/mlld

Presented to the Cold Fusion Workshop Phenomena May 1984

Sante Fe, NM.

COLD FUSION EXPERIMENTS USING MAXWELLIAN PLASMAS AND SUB-ATMOSPHERIC DEUTERIUM GAS

By

Mark Prelas, Frederick Boody, Warren Gallaher,
Edbertho Leal-Quiros, David Mencin, and Scott Taylor

Fusion Research Laboratory
Nuclear Engineering Program
University of Missouri
Columbia, MO 65211

New Energy Times Archive

Experiments are being performed to initiate the cold fusion process in Maxwellian plasmas and sub-atmospheric deuterium gas. Thus far, neutron counts have been observed using a BF₃ probe and Ludlum model 2200 digital counter, and a broad 8.1 MeV peak has been observed using a 3 inch sodium iodide crystal and a Nucleus PCA II multichannel analyzer. The results appear to be dependent upon the temperature of the palladium sample, deuterium pressure, and the type of palladium sample used.

The results are interesting but not sufficient for any conclusions at this point.

Experimental Setup

- The **Modified Missouri Magnetic Mirror Experiment (M4X)** is used as the source for the Maxwellian plasma and as the pressure vessel for the sub-atmospheric deuterium tests.
- The diagnostic package used for the cold fusion work includes:

BF₃ probe with Ludlum model 2200 digital counter for neutron detection

Sodium Iodide detector with a Nucleus PC II MCA for gamma spectroscopy

Two Geiger counters to measure gamma rays

Gold foils for neutron detection

Langmuir Probes for electron temperature, density, and distribution function measurements

Variable Energy Analyzer for ion temperature, density, and distribution function measurements

Thermocouples on both the palladium sample and the BF₃ probe

Bolometer for charged particle measurements

Residual Gas Analyzer for gas analysis

Helium Leak Detector for He detection

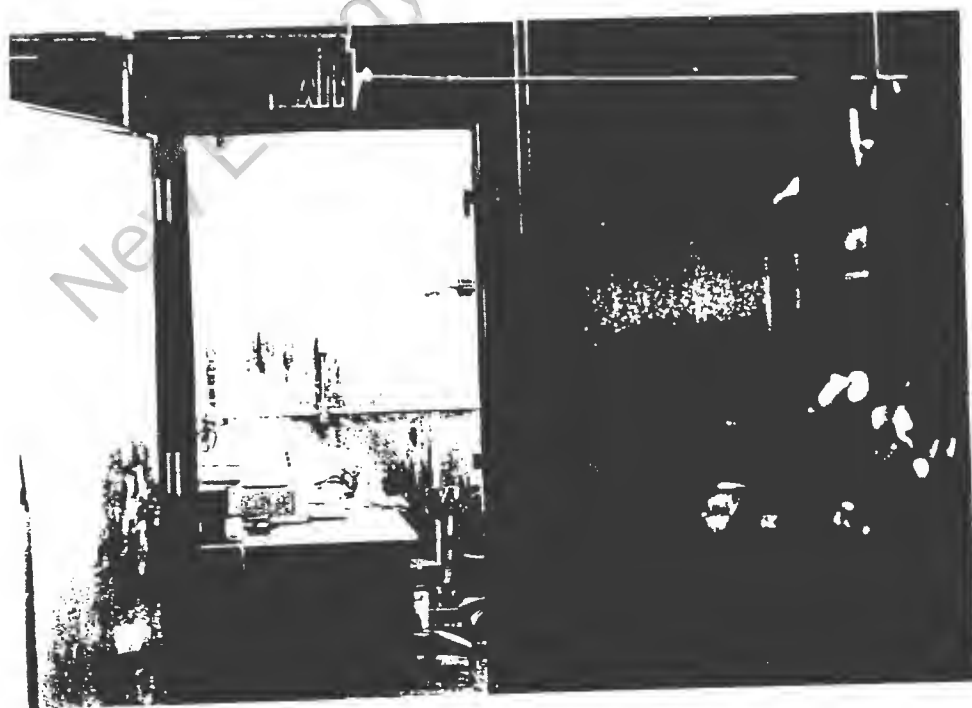
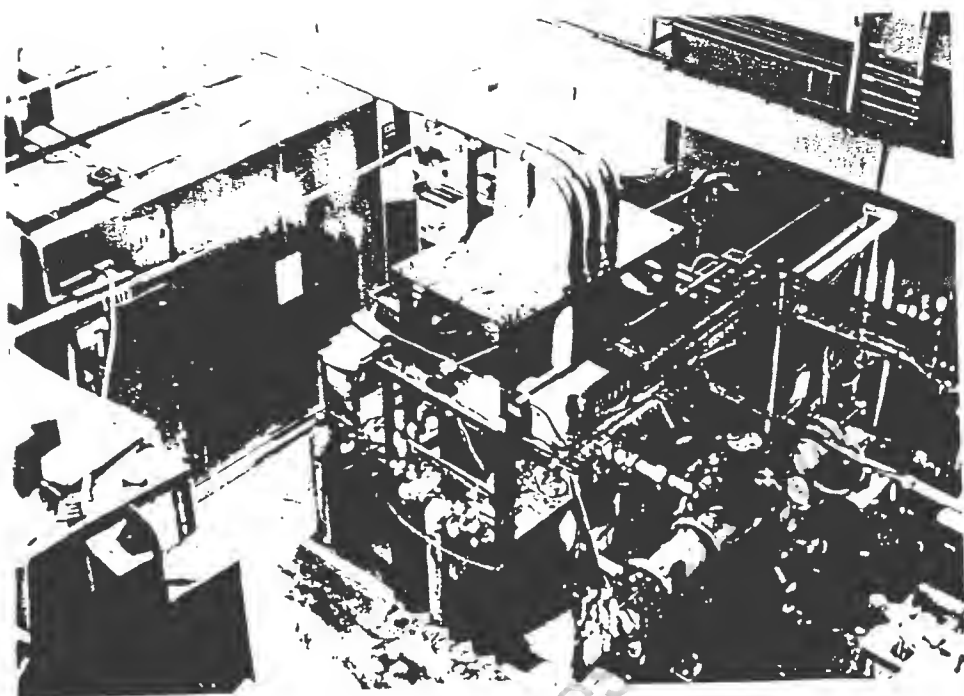
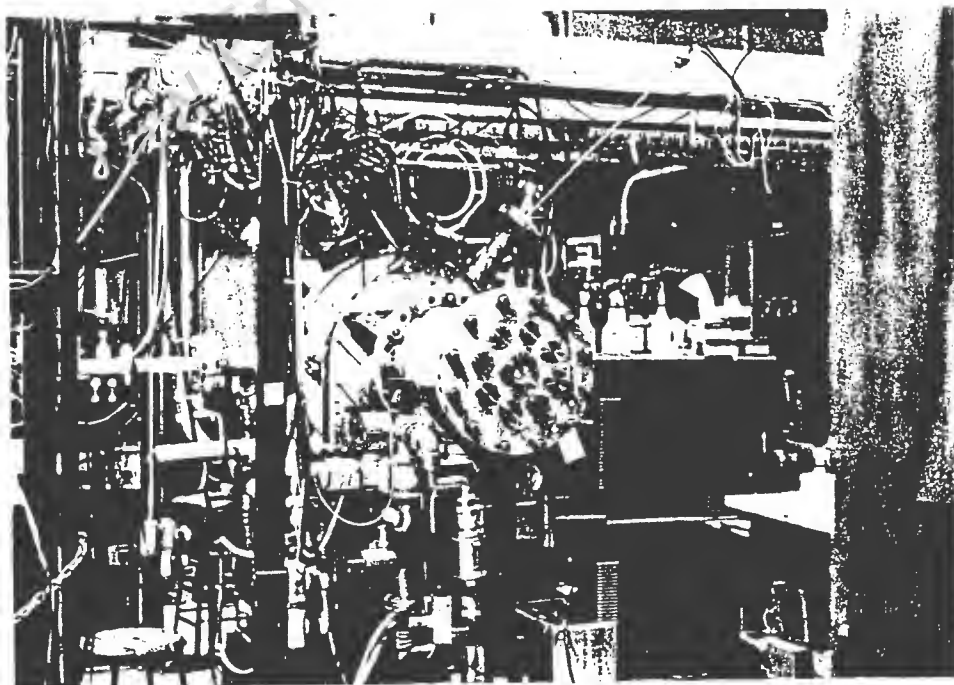
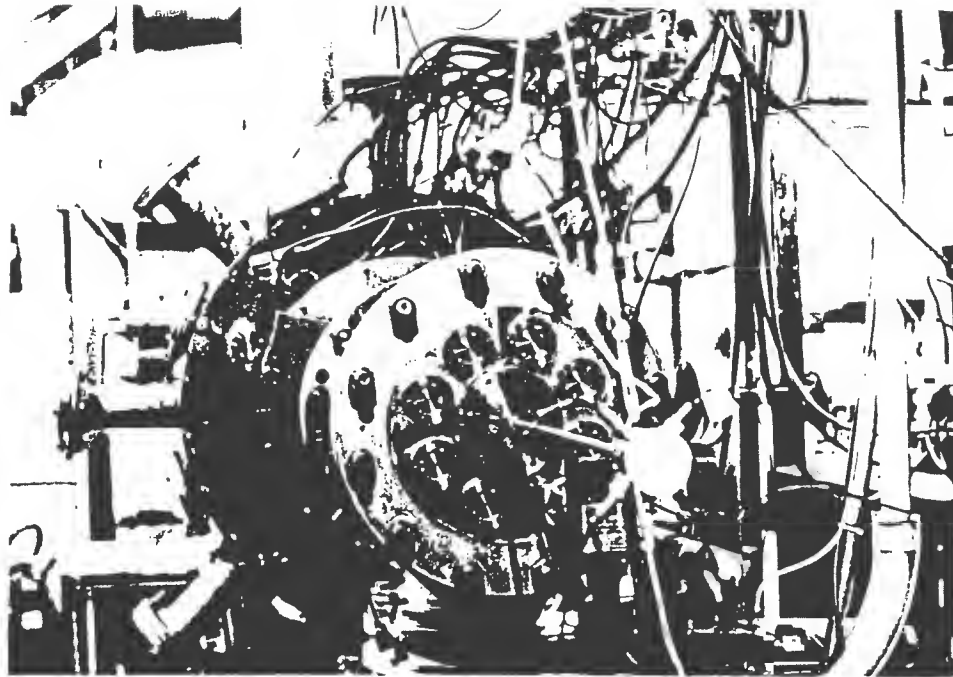
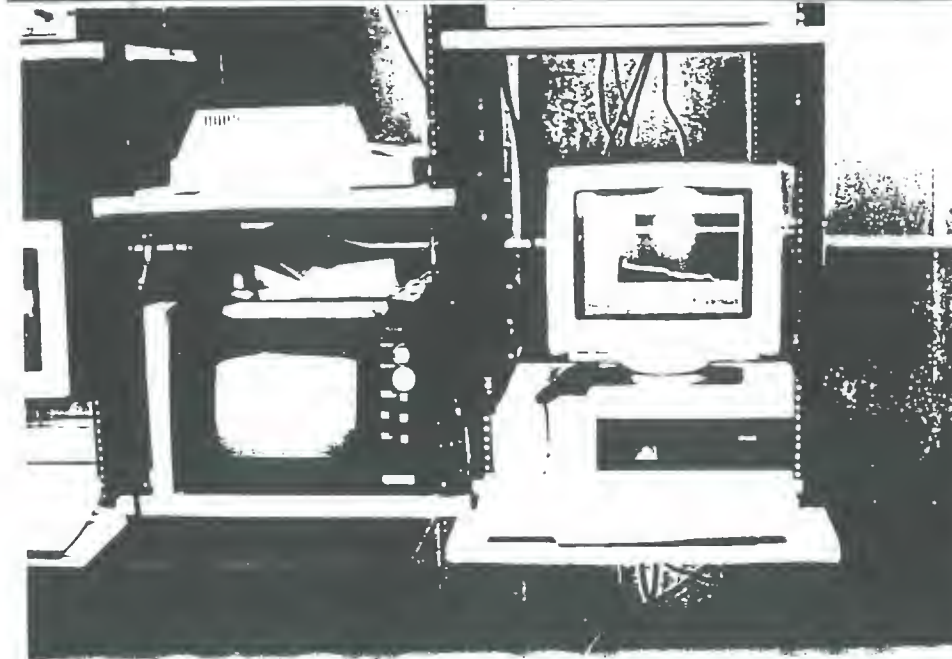
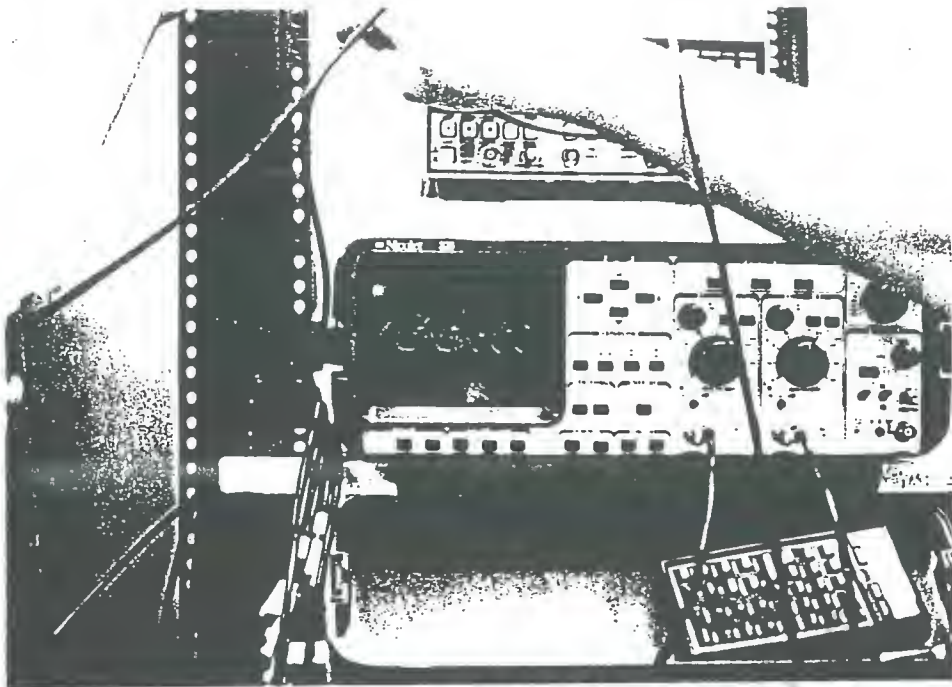


FIG 1 X





The M⁴X is a microwave heated plasma device capable of generating a wide range of plasma conditions and is a recent upgrade of the Missouri Magnetic Mirror Prototype eXperiment (M³PX). The differences between the two devices is shown in Table 1. (It should be noted that by varying microwave power the bulk electron temperature can vary from 1 eV to 10 eV and the bulk ion temperature from 0.5 eV to 10 eV.) This new experimental device, the M⁴X, uses water cooled copper coils. The M⁴X device has incorporated an upgrade to the coil power supplies which allows electron cyclotron resonance heating with a 10.5 GHz, 10 kilowatt power supply obtained on surplus in addition to the 2.45 GHz, 2.5 kW power supply already being used. Some additional work has been done on the vacuum vessel of this device which improves the conductance to the vacuum pumps, and improves diagnostic accessibility. Additionally, a 10 kilowatt tuneable RF power supply (2 to 5 MHz) has been added for ion cyclotron resonance heating experiments. The availability of the electron cyclotron resonance heating and the ion cyclotron resonance heating will provide a variety of ion temperatures. Additionally, the vacuum vessel of the M⁴X has a gas manifold which will allow a choice of ion masses.

Table 1. Comparison of parameters for the M³PX and the M⁴X.

Parameter	M ³ PX	M ⁴ X
r ₁ (radius of point cusp)	0.15 meter	0.15 meter
r ₂ (radius of line cusp)	0.42 meter	0.42 meter
w (width of line cusp)	0.13 meter	0.13 meter
max B _r	0.1 Tesla	0.4 Tesla
max B _z	0.17 Tesla	0.68 Tesla
ECR Heating (2.5 GHz)	2.5 kW	2.5 kW
ECR Heating (10.5 GHz)	0 kW	10 kW
ICR Heating (0.1- 2 MHz)	1 kW	1 kW
ICR Heating (2 - 5 MHz)	0 kW	10 kW
Plasma Density	10 ¹⁶ m ⁻³	10 ¹⁸ m ⁻³
Hot Electron Temp.	15 keV	500 keV
Bulk Electron Temp.	1 to 2.5 eV	1 to 5 eV
Hot Ion Temp.	1 keV	15 keV
Bulk Ion Temp.	0.5 to 5 eV	0.5 to 10 eV
Plasma Volume	9 liters	9 liters

Data Acquisition

The VEA, Bolometer, Langmuir Probe, Thermocouples, and machine status (Magnet current, microwave power, vacuum) were all taken on a digital data acquisition system. Analog signals were channeled to a Bi Ra 5909 32 channel A/D converter in a CAMAC crate then loaded via GPIB to a Macintosh II. Data on the actual current to the probe was also taken in this fashion. Initial analysis and storage was accomplished with Labview software developed by National Instruments. All other data was taken manually and recorded in bound notebooks.

New Energy Times Archive

Experiment #1, 3/27 to 4/16

- Palladium tubing crushed into the shape of a flat rectangular disk (7 mm by 7 mm by 0.25 mm)
- The palladium was mounted in a very special design using a nickel grid to enhance ion current to the palladium
- The palladium sample was placed in the point of the M4X operating in the mirror mode
- A base pressure of 9×10^{-7} Torr was established on the palladium sample for 24 hrs
- A low Ar flow rate was established in the M4X
- A plasma was formed with microwave heating
- Background neutron readings were taken
- A low D₂ flow rate was established in the M4X
- Neutron and gamma ray readings were taken

The cold fusion target was designed to fit into the mirror field point of the M4X as shown in Figure 1.

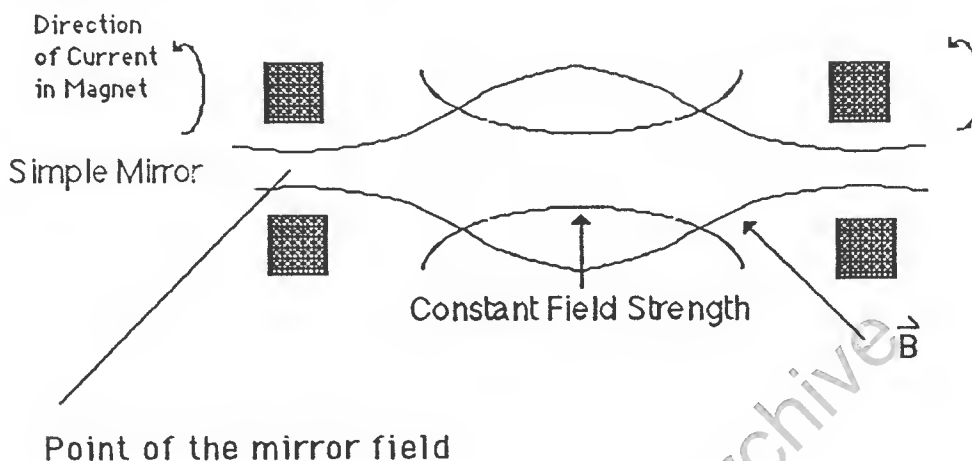


Figure 1. Location of the Mirror field point.

The target was designed to have the optimum capability to collect ions. Using a simple electrode like a Langmuir probe would lead to low ion currents due to Debye shielding effects. Therefore the Fusion Research Laboratory's expertise in ion energy analyzers was used to design a grided target which collects several orders of magnitude greater current than a Langmuir probe or an electrode. The design is shown in Figure 2.

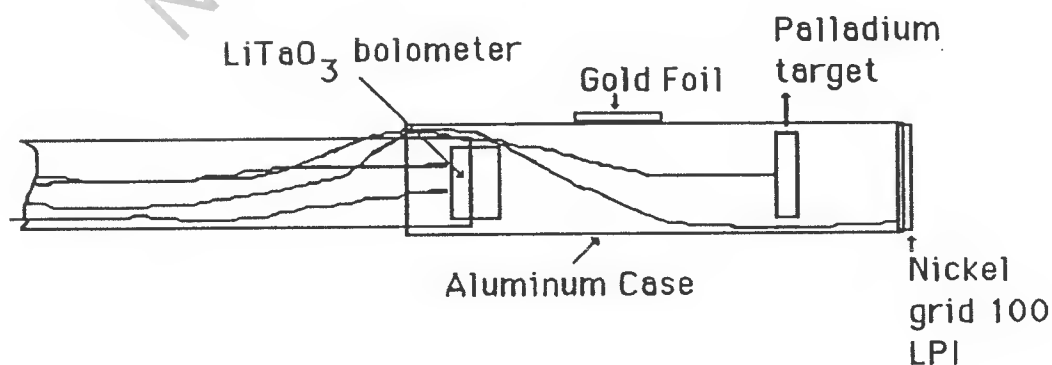
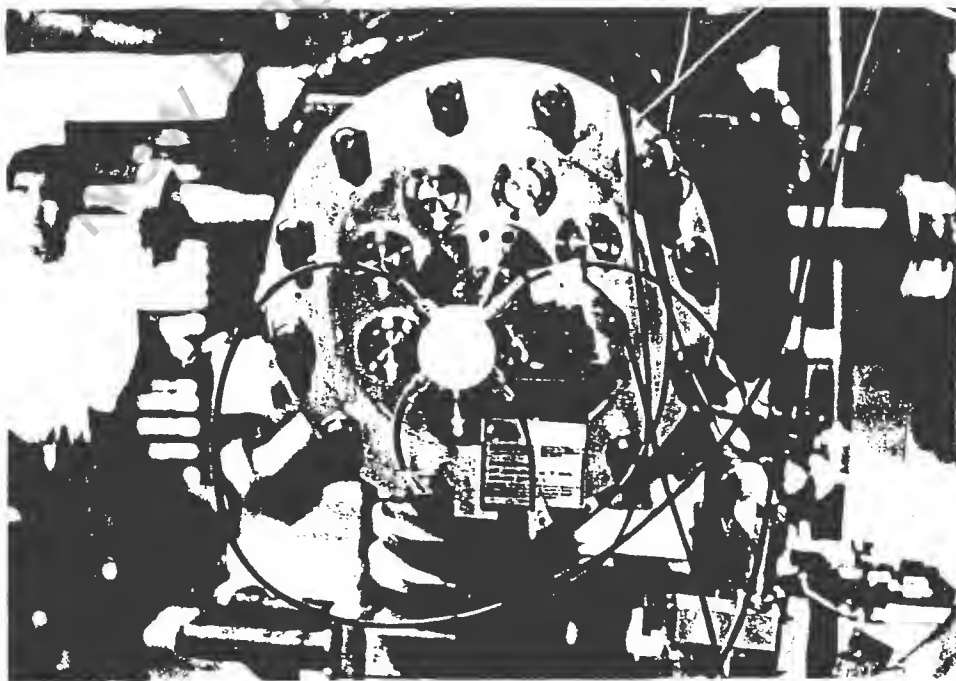
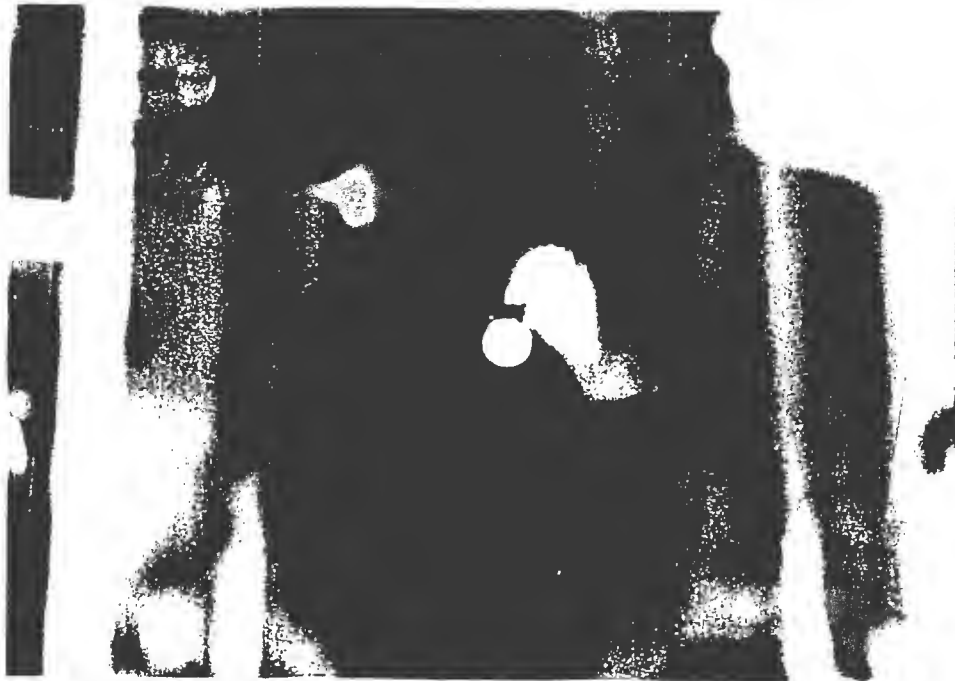


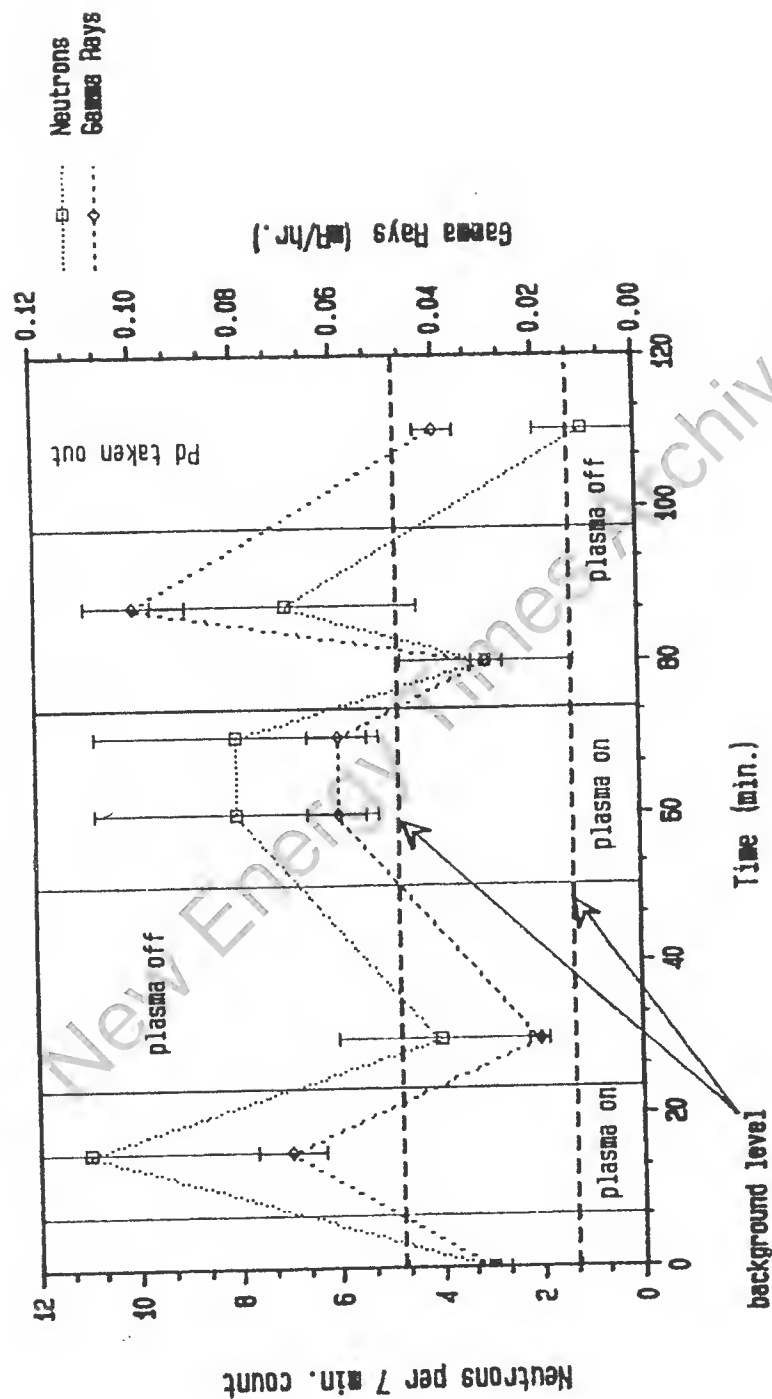
Figure 5. Design of the target used in our cold fusion experiment.

Cold Fusion Target (Pd)

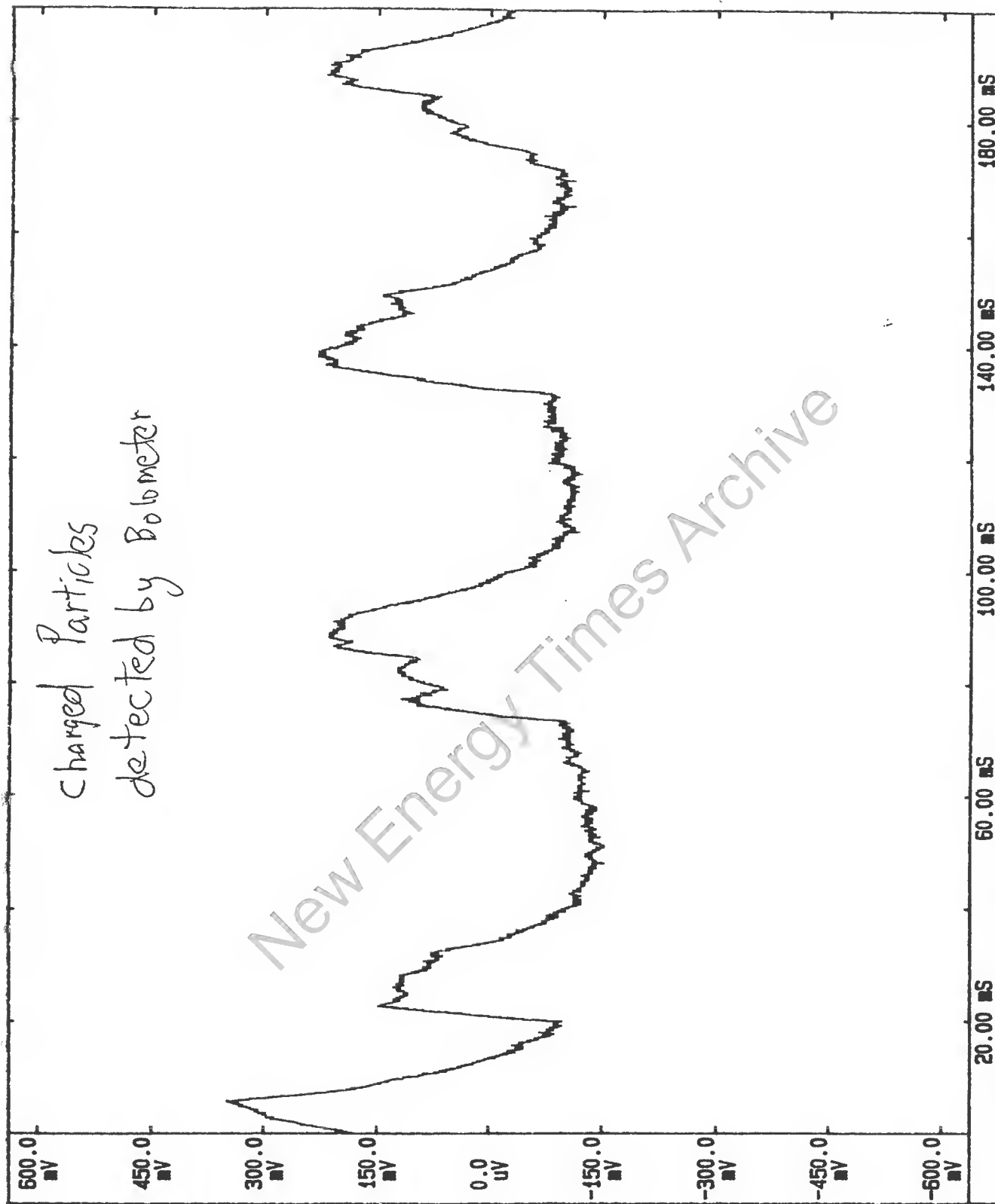


Cold Fusion target in M4X

Experiment #1, 3/27 to 4/16/89



Charged Particles
detected by Bobmeter



Summary of Results from Experiment #1

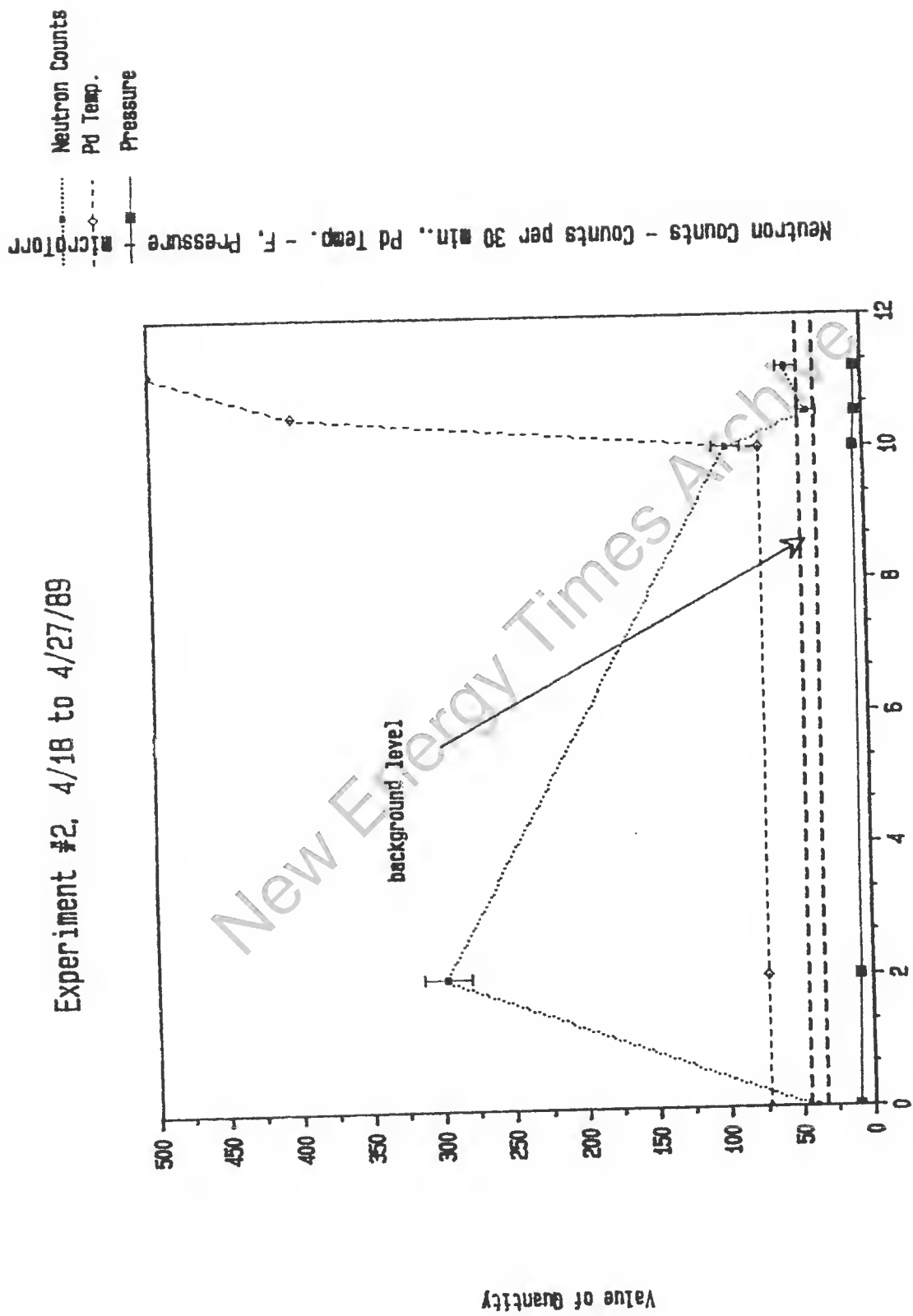
- Apparent neutron readings above background were measured during a plasma discharge and after a plasma discharge
- Apparent gamma ray readings above background were measured after a plasma discharge

New Energy Times Archive

Experiment #2, 4/17 to 4/27

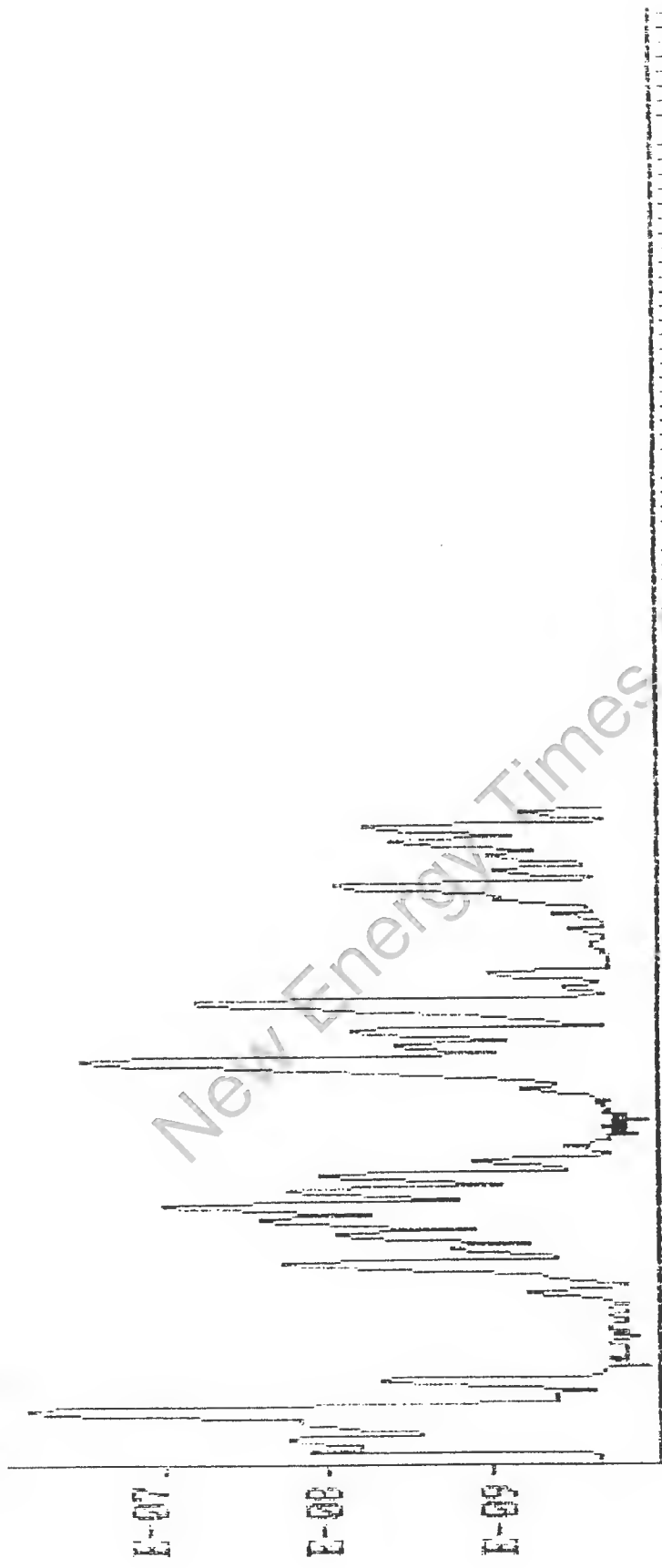
- A new sample of palladium was made from crushed palladium tubing (7 mm by 7 mm by 0.25 mm)
- The palladium sample was put into the M4X
- Background readings were taken with Ar and D₂ plasma while the sample was being built
- The M4X achieved a base pressure of 7×10^{-7} for 48 hrs
- During pumpdown, neutron readings were made. Neutrons were being produced at copious rates of 9.9 neutrons per min for 9 hours.

Experiment #2, 4/18 to 4/27/89



100 PRES 6.4E-06 DISP SPEC A SCAN SPEC A 4/27/89 18:45

4.0E-06



RS-232
BAUD RATE 1200
DATA BITS 8
STOP BITS 2

PRINTER
1200

PARITY
PROTOCOL

ECHO
DELTA_D

40 NONE
DTR ON
6.50 MONTH

50 HOURS
MINUTES
DAY

60

70 8. YEAR
10. FIL PROT
2. MULT VOLT
3. DELTA D

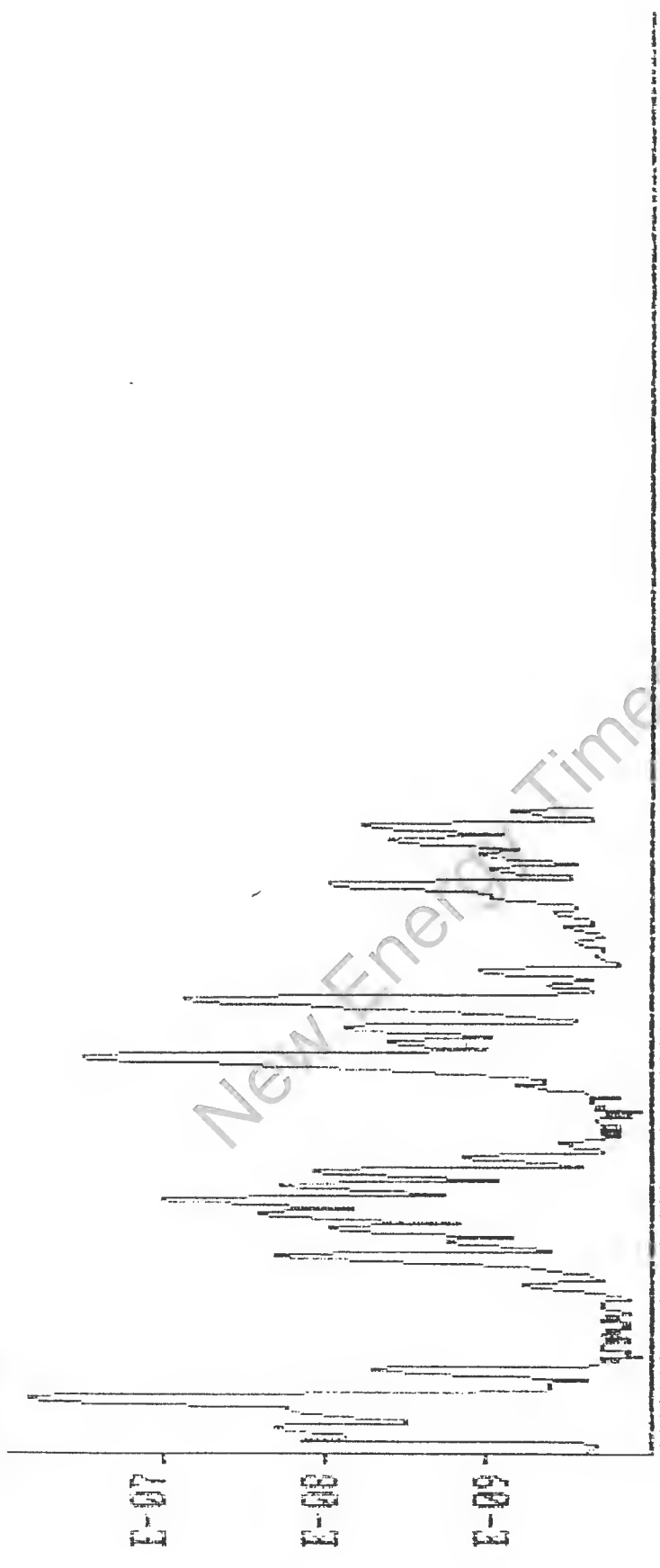
90 100

1.0E-03
-655.
ANALOG

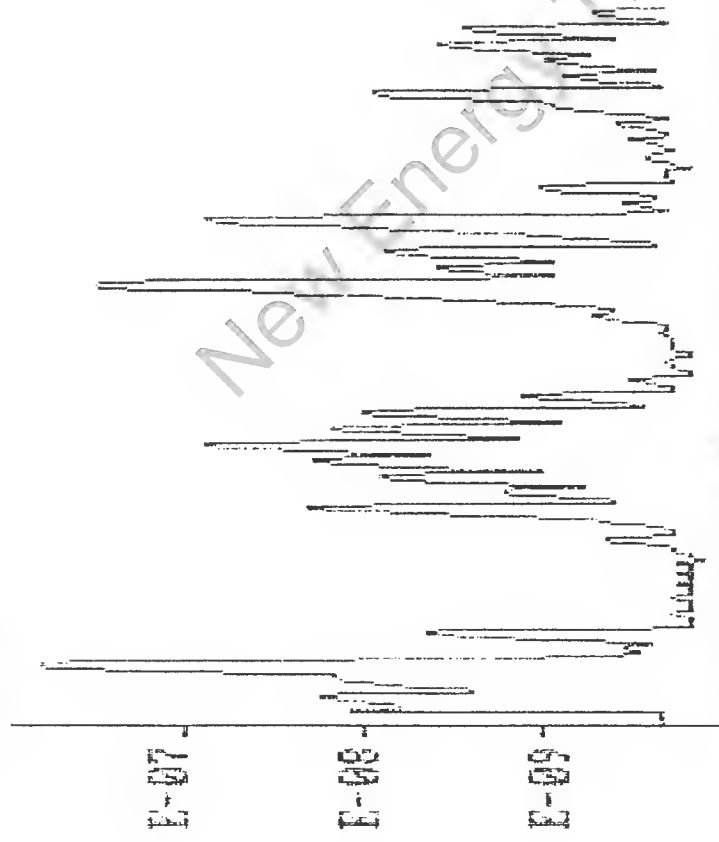
6

TOT PRES 0.82-06 DISF SPEC A SCAN SPEC A 9/27/89 18:55

4.0E-06



LO MASS	10	20	30	40	50	60	70	80	90	100
HI MASS		1. DWELL		15 MSEC	EMISSION	1.0E-03	FIL RES			
SAMP/AML		45. SCALE	4 DEC LOG	EL ENERGY	-70.1	FIL VOLTS				
NO. SCANS		6.	FOCUS	-32.0	FIL CUR					
		-1. AUTO ZERO	OFF	ELEC MULT	ON					



22

— 23 —



USA

1. The first step is to identify the problem or question that needs to be addressed. This involves understanding the context and the specific requirements of the task.

[Illegible vertical text]

THE

THE

10

22



3



DIS

EL ENERGY

FOCUS

[illegible]

THE

11-11-11

Figure 1

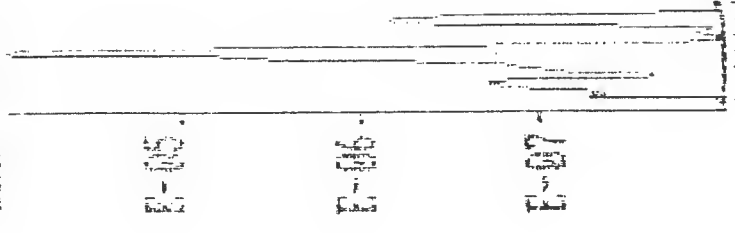
STYLISH

1.
 2.
 3.
 4.
 5.
 6.
 7.
 8.
 9.
 10.
 11.
 12.
 13.
 14.
 15.
 16.
 17.
 18.
 19.
 20.
 21.
 22.
 23.
 24.
 25.
 26.
 27.
 28.
 29.
 30.
 31.
 32.
 33.
 34.
 35.
 36.
 37.
 38.
 39.
 40.
 41.
 42.
 43.
 44.
 45.
 46.
 47.
 48.
 49.
 50.
 51.
 52.
 53.
 54.
 55.
 56.
 57.
 58.
 59.
 60.
 61.
 62.
 63.
 64.
 65.
 66.
 67.
 68.
 69.
 70.
 71.
 72.
 73.
 74.
 75.
 76.
 77.
 78.
 79.
 80.
 81.
 82.
 83.
 84.
 85.
 86.
 87.
 88.
 89.
 90.
 91.
 92.
 93.
 94.
 95.
 96.
 97.
 98.
 99.
 100.



TOT PRES 3.6E-05 DISP SPEC 15000 SPEC 14733

TIME 01-04



New Energy Times

LO MESS
HI MESS
SCAN/AND
NO. SCANS

10 20 30 40 50 60 70 80 90 100
1. IDUELL 1.0E-03 FIL RES
45. SCALE -70.1 FIL VOLTS
6. FOCUS -32.0 FIL CUR
-1. AUTO ZERO OFF FELEC MULT ON

Summary of Results from Experiment #2

- Apparent neutron counts were measured in a low pressure deuterium gas (about 1×10^{-5} Torr)

Counts can be produced at sub-Torr pressures

- As the sample was being heated, the neutron counts quickly dropped to background level

There is a potential temperature effect where lower temperatures favor apparent neutron counts.

New Energy Times Archive

Experiment #3, 5/12 to 5/20

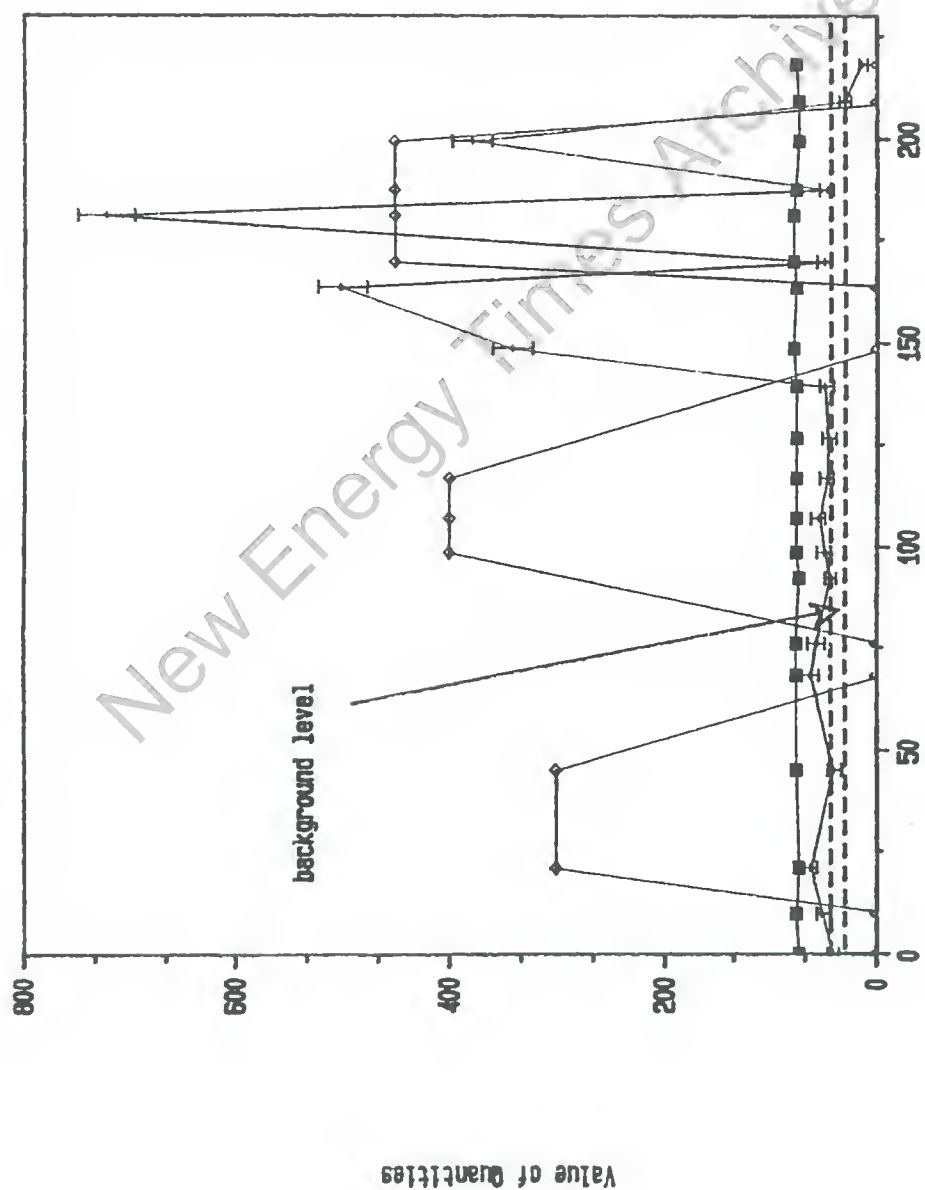
- A palladium foil was purchased and used (25.4 mm by 25.4 mm by 0.5 mm)
- Both plasma and pressure were used to initiate the neutron counts
- Neutron counts were observed at both relatively high D₂ pressure and very low D₂ pressure

New Energy Times Archive

Experiment #3 5/12/89 to 5/20/89

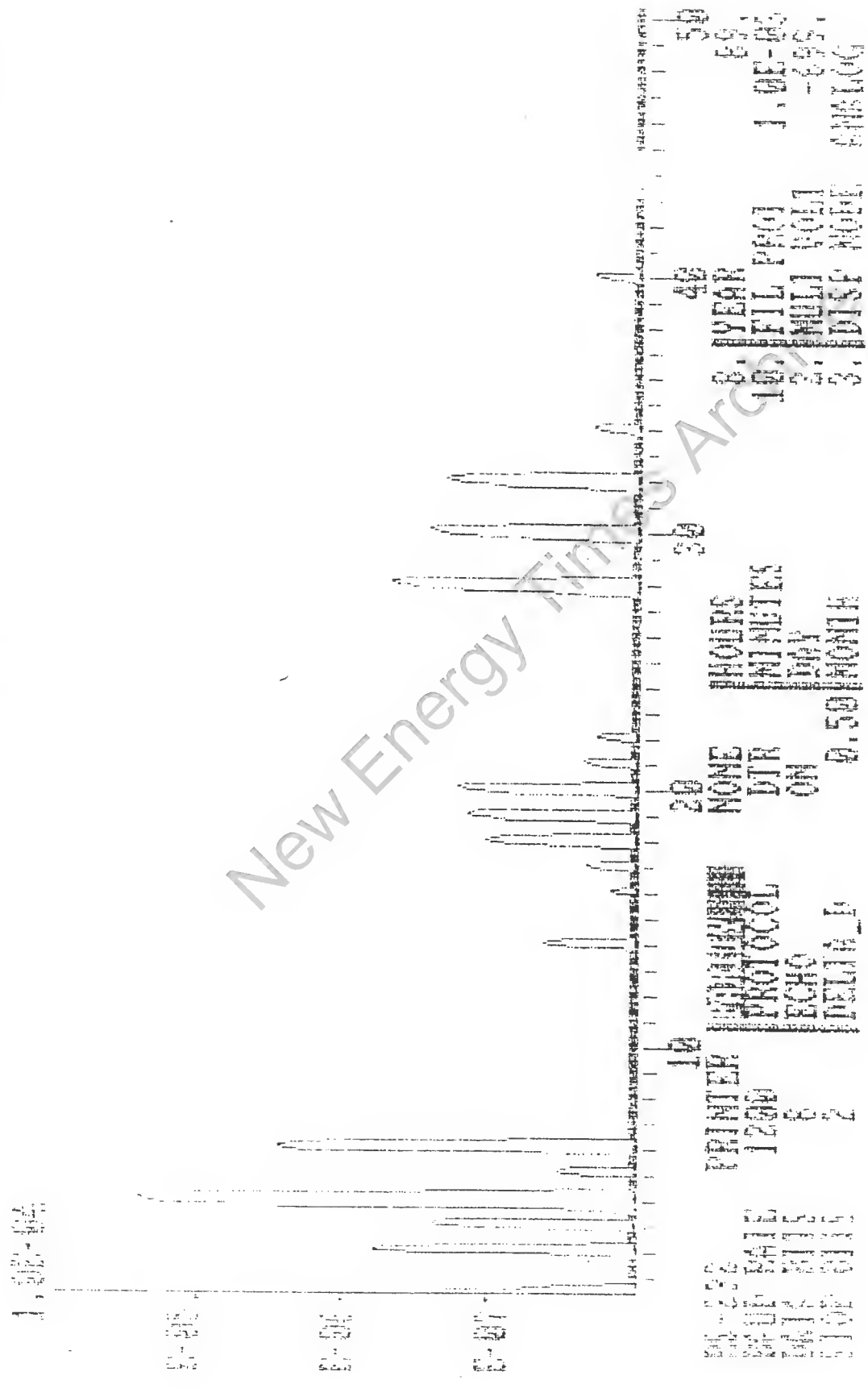
Neutrons
Pressure
Temperature

Neutrons-counts per 500 min., Pressure-Torr, Temperature-F



Time (hr.)

IN 345 2.25-04.00 REC 4 15.00-04.00 REC 4 2.00-04.00 REC 4 2.00-04.00 REC 4

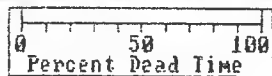


Nucleus FCA-II

11:12:38 PM May 19, 1989

May 21, 1989
2:59:34 PMAcquire: Off
Mode: PHA
Timer: Live
Scale: Log
Group: Full
Roi No: None
Roi: Off
Gain: 4096
Offset: 8
Ade: Add
Display: 4096
Overlap: OffMeV: 1.52
Cts: 448

Preset: 0 Elapsed: 0 Real: 19594


Percent Dead Time

Filename: b519218.pmd

F1-Acquire F2-Erase F3-Preset F4-Expand F5-Ident F6-Load F7-Save Esc-R01

May 21, 1989

3:17:11 PM

Acquire: Off

Mode: PHA

Timer: Live

Scale: Log

Group: Full

ROI No: None

ROI: On

Gain: 4096

Offset: 0

ADC: Add

Display: 4096

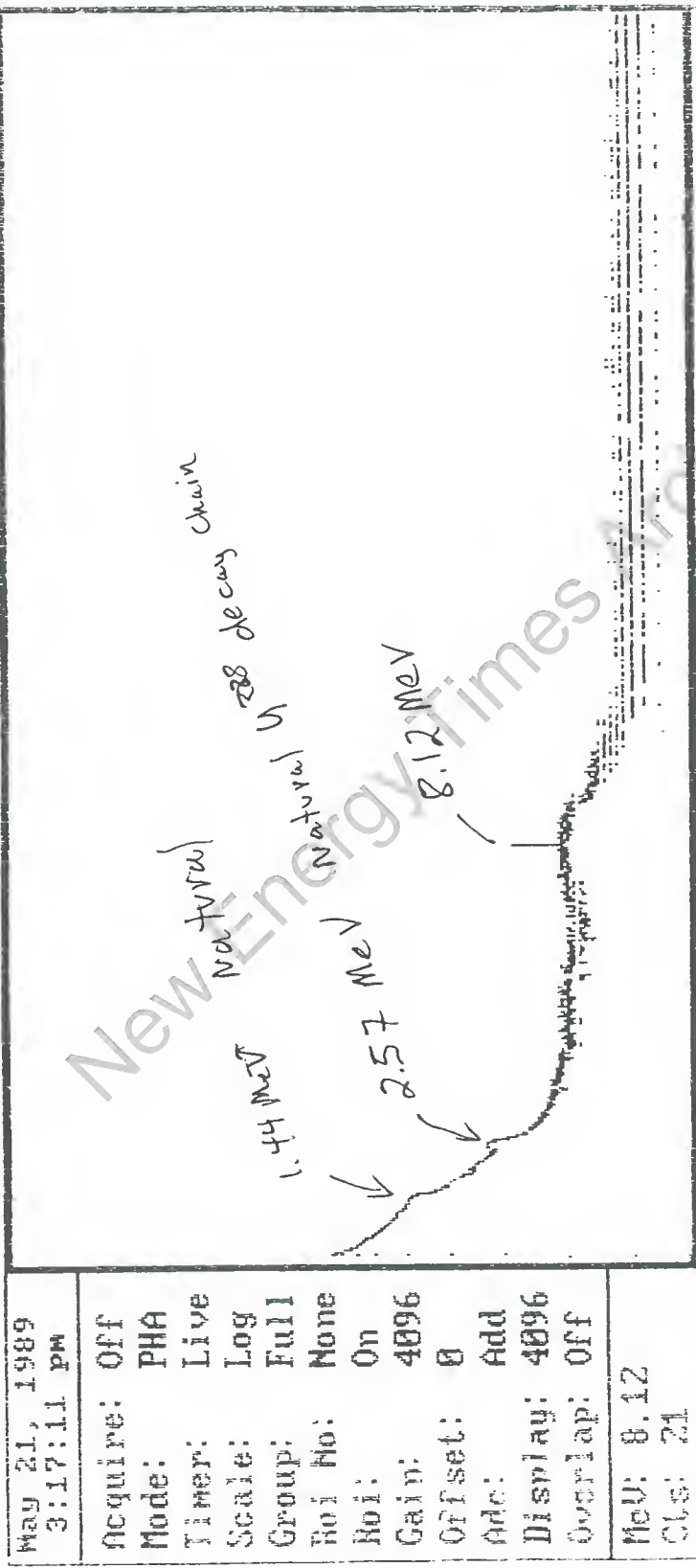
Overlap: Off

MeV: 8.12

CLS: 21

04:02:37 AM May 20, 1989

Nucleus PCA-II



Preset: 0

Elapsed: 0

Real: 30180

Percent Dead Time

0 50 100

Figure 1 illustrates the stages of chick development from fertilization to hatching. The sequence includes: 1. Fertilized egg, 2. Cleavage stages, 3. Blastoderm, 4. Yolk sac formation, 5. Embryo development, 6. Hatching process, 7. Hatched chick, 8. Yolk sac, 9. Chick in the nest, 10. Chick in the nest, 11. Chick in the nest, 12. Chick in the nest.

$\frac{1}{n} \sum_{i=1}^n x_i = \bar{x}$

ॐ नमो भगवते वासुदेवाय
 ॐ नमो भगवते वासुदेवाय
 ॐ नमो भगवते वासुदेवाय
 ॐ नमो भगवते वासुदेवाय
 ॐ नमो भगवते वासुदेवाय

[Faint musical notation]

1. The first part of the text discusses the importance of maintaining accurate records of all transactions, including sales, purchases, and expenses. It emphasizes that this is crucial for determining the correct amount of tax to be paid.

... ..

Figure 1 is a schematic representation of the experimental design. It shows a sequence of steps: 1. A subject is shown in a box labeled 'Subject'. 2. An arrow points to a box labeled 'Stimulus presentation'. 3. An arrow points to a box labeled 'Response'. 4. An arrow points to a box labeled 'Feedback'. 5. An arrow points to a box labeled 'Next trial'. The sequence is enclosed in a larger box labeled 'Trial'.

[illegible]

— — —
3-5-2

—

15

[illegible]

7

100

1. *Staphylococcus aureus*
2. *Staphylococcus aureus*
3. *Staphylococcus aureus*
4. *Staphylococcus aureus*
5. *Staphylococcus aureus*
6. *Staphylococcus aureus*
7. *Staphylococcus aureus*
8. *Staphylococcus aureus*
9. *Staphylococcus aureus*
10. *Staphylococcus aureus*

426

100



1. 1. The first
 2. 2. The second
 3. 3. The third
 4. 4. The fourth
 5. 5. The fifth
 6. 6. The sixth
 7. 7. The seventh
 8. 8. The eighth
 9. 9. The ninth
 10. 10. The tenth
 11. 11. The eleventh
 12. 12. The twelfth
 13. 13. The thirteenth
 14. 14. The fourteenth
 15. 15. The fifteenth
 16. 16. The sixteenth
 17. 17. The seventeenth
 18. 18. The eighteenth
 19. 19. The nineteenth
 20. 20. The twentieth
 21. 21. The twenty-first
 22. 22. The twenty-second
 23. 23. The twenty-third
 24. 24. The twenty-fourth
 25. 25. The twenty-fifth
 26. 26. The twenty-sixth
 27. 27. The twenty-seventh
 28. 28. The twenty-eighth
 29. 29. The twenty-ninth
 30. 30. The thirtieth
 31. 31. The thirty-first
 32. 32. The thirty-second
 33. 33. The thirty-third
 34. 34. The thirty-fourth
 35. 35. The thirty-fifth
 36. 36. The thirty-sixth
 37. 37. The thirty-seventh
 38. 38. The thirty-eighth
 39. 39. The thirty-ninth
 40. 40. The fortieth
 41. 41. The forty-first
 42. 42. The forty-second
 43. 43. The forty-third
 44. 44. The forty-fourth
 45. 45. The forty-fifth
 46. 46. The forty-sixth
 47. 47. The forty-seventh
 48. 48. The forty-eighth
 49. 49. The forty-ninth
 50. 50. The fiftieth
 51. 51. The fifty-first
 52. 52. The fifty-second
 53. 53. The fifty-third
 54. 54. The fifty-fourth
 55. 55. The fifty-fifth
 56. 56. The fifty-sixth
 57. 57. The fifty-seventh
 58. 58. The fifty-eighth
 59. 59. The fifty-ninth
 60. 60. The sixtieth
 61. 61. The sixty-first
 62. 62. The sixty-second
 63. 63. The sixty-third
 64. 64. The sixty-fourth
 65. 65. The sixty-fifth
 66. 66. The sixty-sixth
 67. 67. The sixty-seventh
 68. 68. The sixty-eighth
 69. 69. The sixty-ninth
 70. 70. The seventieth
 71. 71. The seventy-first
 72. 72. The seventy-second
 73. 73. The seventy-third
 74. 74. The seventy-fourth
 75. 75. The seventy-fifth
 76. 76. The seventy-sixth
 77. 77. The seventy-seventh
 78. 78. The seventy-eighth
 79. 79. The seventy-ninth
 80. 80. The eightieth
 81. 81. The eighty-first
 82. 82. The eighty-second
 83. 83. The eighty-third
 84. 84. The eighty-fourth
 85. 85. The eighty-fifth
 86. 86. The eighty-sixth
 87. 87. The eighty-seventh
 88. 88. The eighty-eighth
 89. 89. The eighty-ninth
 90. 90. The ninetieth
 91. 91. The ninety-first
 92. 92. The ninety-second
 93. 93. The ninety-third
 94. 94. The ninety-fourth
 95. 95. The ninety-fifth
 96. 96. The ninety-sixth
 97. 97. The ninety-seventh
 98. 98. The ninety-eighth
 99. 99. The ninety-ninth
 100. 100. The hundredth

[Faint, illegible handwritten notes or bleed-through from the reverse side of the page.]



THE
JOURNAL OF THE
ROYAL ANTHROPOLOGICAL INSTITUTE

4

[illegible]
$$L_{\alpha}^{\pm} = \frac{1}{2} (L_{\alpha} \pm iM_{\alpha})$$

352K

(Alt) Help File Calc Setup Options Mode Quit

Nucleus PCA-II 2:14:14 pm May 20, 1989

May 21, 1989
3:11:37 pm

Acquire: Off
Mode: PHA
Timer: Live
Scale: Log
Group: Full
Roi No: None
Roi: Off
Gain: 4096
Offset: 0
Ade: Add
Display: 4096
Overlap: Off

Chn: 212
Cls: 588

Preset: 0

Elapsed: 0

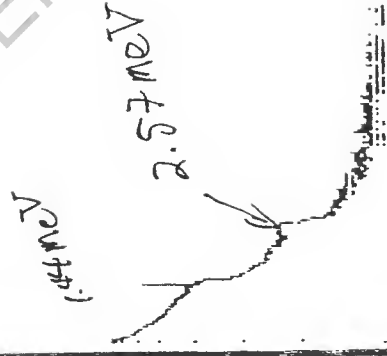
Real: 28553

0 50 100
Percent Dead Time

Filename: b5201010.pmd

F1-Acquire F2-Erase F3-Preset F4-Expand F5-Ident F6-Load F7-Save Esc-ROI

New Energy Times



Summary of Results from Experiment #3, 5/12 to 5/22

- The neutron count rates were enhanced by both low and high pressure D₂
- There appears to be cyclic behavior in the neutron count rate (counts were staggered between day, evening, and early morning)
- An unusual 8.1 MeV peak was observed on one of the experimental runs.

New Energy Times Archive

Acknowledgements

The authors wish to thank the National Science Foundation (Grant # NSF CBT-8352345; Presidential Young Investigator Award), and the McDonnell Douglas Foundation for their support of this project. Additionally, the authors are indebted to Prof. William H. Miller for help with the neutron calibration, Dr. Brad Keck for help with the gamma ray spectrometer, to Jalal Javidani for helping to take data, to Ms. Rosemary Roberts P.E., Prof. Jay Kunze, Dr. Chris Wallace, Prof. Aaron Krawitz, Prof. George Miley & Prof. Albert Gu for many useful discussions, to the UMC Chemistry Dept. for loaning us a palladium sample, to UMC's Health Physics Department for loaning us a BF_3 probe, and an MCA, and to Memoree DeSpain for assisting us with acquisition of vital materials for this research.

New Energy Times Archive

Energy Research Advisory Board
to the
United States Department of Energy
1000 Independence Avenue, S.W.
Washington, D.C. 20585
(202) 586-5444

U SEP 89 9. 93

-R.L. GARDIN-


September 1, 1989

Subject: Chairman's July 20 Request for Summaries of Past and Present Cold Fusion Research and August 9 Request for Tritium Production Results

The following have been received to date from the following individuals in response to the above requests:

- H. L.R. Greenwood, ANL (response to August 9 request)
- I. F. Besenbacher, University of Aarhus (response to July 20 request)
- J. N.J.C. Packham (for Bockris), Texas A&M (response to August 9 request)
- K. J. Paquette, Atomic Energy of Canada, Ltd.

Immediately behind this memorandum is a cumulative index.


William L. Woodard
Panel Secretary

Enclosures

New Energy Times Archive

INDEX

- A. Bo U.R. Sundquist, Uppsala University (response to both requests)
- B. W. Scheid, Giessen University (responses to both requests)
- C. M.M. Broer, AT&T Bell Laboratories (response to August 9 request)
- D. J. Eridon, Naval Research Laboratory (response to August 9 request)
- E. Y.E. Kim, Purdue University (response to July 20 request)
- F. A Schriesheim, Argonne National Laboratory (response to July 20 request)
- G. M.A. Prelas, University of Missouri, Columbia
- H. L.R. Greenwood, ANL (response to August 9 request)
- I. F. Besenbacher, University of Aarhus (response to July 20 request)
- J. N.J.C. Packham (for Bockris), Texas A&M (response to August 9 request)
- K. J. Paquette, Atomic Energy of Canada, Ltd.

ARGONNE NATIONAL LABORATORY

9700 SOUTH CASS AVENUE, ARGONNE, ILLINOIS 60439

Telephone: (312)972-4351

August 23, 1989

J. R. Huizenga
Co-Chairman, ERAB
Panel on Cold Fusion
ER-6 3F-061
U.S. Department of Energy
1000 Independence Avenue, S.W.
Washington, D.C. 20585

Dear Mr. Huizenga:

I have been asked to reply to your letter of August 9 regarding our tritium measurements in electrolytic cells during our "cold fusion" experiments at Argonne. The enclosed summary answers the questions in your letter based on experiments conducted by C. A. Melendres and myself during April 1989. The tritium measurements were conducted by D. L. Bowers of our Analytical Chemistry Laboratory. All of our results have been negative in that we have seen no excess heat, no tritium production, and no neutron or gamma production.

If you have any further questions about our measurements, please give me a call.

Sincerely,

Lawrence R. Greenwood

Lawrence R. Greenwood
Chemical Technology Division

LRG:cew
Enclosure

Summary of Tritium Production in "Cold Fusion" Experiments
L.R. Greenwood and C.A. Melendres
Argonne National Laboratory

1. The D_2O used in our experiments was purchased from Aldrich Chemical Co., Milwaukee, WI, in 100 g bottles with an isotopic purity of 99.8% D. Analysis of the initial tritium in the D_2O gave a rate of 70 dpm/ml corresponding to a tritium/deuterium ratio of 9.0×10^{-15} or 6.7×10^8 atoms of tritium/ml of D_2O . LiOD was added to the solution; however, no additional tritium was detectable due to the LiOD.

2. The electrolytic cell was a standard H-type glass cell with the anode and cathode compartments separated by a medium porosity glass frit. A third compartment housed a calomel reference electrode with a Luggin capillary bridge to the Pd cathode. The D_2O volume was about 90 ml. Various Pd cathodes were used consisting of foils, cylinders, and wires (see Table I). The longest run used a 1 mm od by 10.6 cm wire of Pd.

3. Operating conditions for a number of experiments are listed in Table I. For the longest run (6) at a current density of 125 mA/cm^2 , the solution was 0.5 M LiOD in D_2O . The experiment was run for 144 hours. The temperature in the working electrode compartment varied from 40 to 60°C during the course of the experiment. D_2O loss was replenished.

4. D_2O was added to the cell three times a day, in the morning, at midday, and late in the afternoon. The volume added varied from a few cc up to 10-15 cc.

5. Tritium analyses were performed by liquid scintillation counting. A 0.1 ml sample was taken from our cell daily and added to a standard liquid scintillation cocktail. Since the LiOD makes a highly basic solution, 0.1 ml of 0.5 M HCL acid was added to neutralize the cocktail prior to analysis. Without this acid addition, chemical luminescence effects may have been seen. The count rate and energy spectrum was then measured with a Packard model 2050CA Liquid Scintillation Analyzer. The background counting rate was 5 counts per minute. The D_2O tritium background was 70 dpm/ml, as given above. No additional tritium was ever detected above our background level. Integrating over the time of our experiments, we can place a limit on the tritium production at less than 100 atoms of tritium per second or 1 t/s/ml of solution.

6a. Neutron Production. Neutron measurements were performed with a boron-loaded liquid scintillator detector measuring 12 cm diameter by 5 cm thick coupled to a 12 cm diameter phototube. ^{10}B -trimethyl borate was added to detect thermal neutrons and fast neutrons could also be detected by proton recoils. Polyethylene bricks were placed around the cell and detector to enhance our chances of detecting a neutron. The detector was located about 7 cm from the center of the cell and we estimate that the net efficiency for 2.5 MeV neutrons was about 15%. Pulse shape discrimination was used to suppress gamma rays. The observed neutron background was about 30 counts per

minute and natural variations in background were observed up to 10% while the electrolytic cell was not in operation. No neutrons were detected above background placing a limit on neutron production of less than 1 neutron per second or 0.01 n/s/ml of solution.

6b. Gamma Production. Gamma measurements were performed with a 7.6 x 7.6 cm NaI detector located at about 7 cm from the center of the cell. An energy window was set for all gammas above 1.9 MeV and the spectra were recorded. The background was determined to be about 100 counts per minute, even with some lead shielding, primarily due to radon (^{214}Bi) and ^{40}K . It was noted that radon decay produces strong gamma lines near 2.2 MeV (2119, 2204, and 2448 keV). Furthermore, the radon background varied strongly from day to day. The polyethylene bricks were also intended to enhance the conversion of neutrons to capture gammas. Using the calculated photoefficiency of NaI as 0.6%, we can say that the gamma production was less than 50 per second or 0.5 gammas/s/ml of solution.

7. No excess heat or tritium was detected.

8. Several other programs in our building use tritium or analyze for tritium routinely. The liquid scintillation detector is also used routinely for tritium analyses.

Additional Comments:

Regarding tritium production, it is possible that preferential evaporation and absorption effects for deuterium could lead to some enhancement of the tritium/deuterium ratio in the cell, especially after prolonged operation. Neutron detection is complicated by the large and strongly varying background. Gamma detection of a 2.2 MeV line could easily be confused with radon, especially due to the strong daily variations in the radon background. Nevertheless, we should have had no difficulty in seeing the production rates reported by M. Fleischmann and S. Pons; however, detection of the much lower rates reported by S. Jones would clearly be more difficult.

ELECTROCHEMICAL DATA

Run	Electrode	Electrolyte	i (mA/cm ²)	Time (hrs)	T(°C)*
1	0.25"Φx0.04"W Pd cylinder	0.2M LiOD/D ₂ O	4.7	25	25
2	0.70"x0.63"x0.025" Pd foil	0.1 M LiF/D ₂ O	1.9	28	26
3	0.040" Pd wire	0.2 M LiOD/D ₂ O	13 mA/cm ² to 130 A/cm ²	short periods <1 hr	-
4	0.040" Pd wire	0.2 M LiOD/D ₂ O	130	1	-
5	0.040" Pd wire	0.2 M LiOD/D ₂ O	13 A/cm ²	1	70-80
6	0.04"Φx4.2" Pd wire	0.5 M LiOD/D ₂ O	125	144	40-60

*in cathode compartment

DET FYSISKE INSTITUT, AARHUS UNIVERSITET
Institute of Physics, University of Aarhus

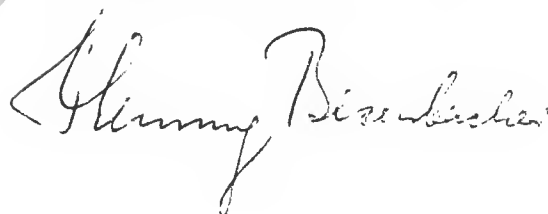
Aarhus, August 23

Dear Dr. Huizenga.

Please find enclosed three papers dealing with cold fusion aspects. Two of them is part of an ongoing program dealing with hydrogen interactions with metals. I am enclosing also an earlier review paper dealing with these aspects.

Sincerely yours

Flemming Besenbacher.

A handwritten signature in cursive script, reading "Flemming Besenbacher".

New Energy Times Archive

SEARCH FOR COLD FUSION IN PLASMA-CHARGED Pd-D AND Ti-D SYSTEMS

F. Besenbacher, B. Bech Nielsen, P. Hornshøj,

E. Lægsgaard, and N. Rud

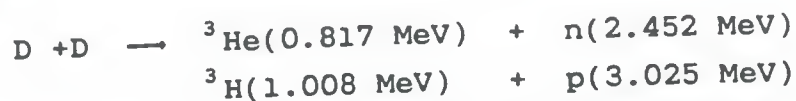
Institute of Physics, University of Aarhus

DK 8000 Aarhus C, Denmark

ABSTRACT

To investigate whether cold fusion of deuterium (D) can occur in solid Pd and Ti as proposed recently, we have searched for the D-D fusion reaction in plasma-charged Pd-D and Ti-D. In a small reaction cell, a DC glow-discharge was established in a deuterium gas between two electrodes, with a Pd or Ti sample placed on the cathode. A thin (50 Å) Cu film was evaporated on the surface of the Pd samples to establish a barrier reducing the escape of D from the samples. Neutrons were detected with a liquid scintillator, and conventional pulse-shape discrimination technique was employed to distinguish gamma counts from neutron counts. No indication for a neutron count rate in excess of the natural background level was observed.

It has recently been suggested [1-3] that cold fusion occurs in hydride-forming metals (Pd and Ti) charged with deuterium (D) in electrochemical cells. The conventional channels for D-D reactions are



Fleischmann, Pons, and Hawkins [1] reported a neutron yield at about 2.5 MeV and at a flux of $4 \times 10^4 \text{ s}^{-1}$ from a 15 g Pd rod, measured with a neutron dosimeter with an efficiency of 2.4×10^{-6} . However the heat generation reported by these authors would require rates from the reactions (1) and (2) which were a factor 10^7 higher. On the other hand, Jones et al [2] detected 2.4 MeV neutrons at rate of only $0.04\text{--}0.06 \text{ s}^{-1}$ [2,3]. With an efficiency of 1% and 3 g Ti, they quoted a "cold fusion rate" for d+d: $\lambda_f \approx 10^{-23}$ fusions/deuteron pair/sec [2,3] and no heat excess.

However, based on our previous studies of D in Pd [3-6] and other metals [5,7-9], we find it difficult to understand why cold fusion should occur. It is known that D occupies the octahedral (O_h) interstitial site in Pd [5,10], and when the atomic concentration of D in the Pd lattice exceeds one, D starts to occupy the tetrahedral (T_h) interstitial sites [10,11]. In addition, D atoms are bound rather strongly to defect traps (e.g., vacancies) and impurities [5,7-9]. In particular, multiple occupancy of vacancies has been observed both theoretically and experimentally (one vacancy can bind up to six D atoms [12-13]). However, irrespective of the D-site occupancy or the occupancy of traps (e.g., vacancies), the D-D distances are always larger than that for the D-D separation in a D_2 molecule (0.74 Å). For

example the distances between two O_h sites in Pd corresponding to D in solid solution are 2.75 Å, between a O_h and a T_h site 1.68 Å, and finally the minimum distance between two D atoms trapped to a vacancy is 1.85 Å [6]. This indicates that the effective D-D interaction of D atoms embedded in the metal is more repulsive than in vacuum, in accordance with a recent effective-medium-theory calculation [11]. Based on existing knowledge of the equilibrium behaviour of the metal-hydrogen system, it thus seems that the probability of tunneling through the Coulomb barrier is approximately 70 orders of magnitude too low to explain the claims of cold fusion.

Jones et al [2], however, argued that cold fusion occurs only if the system is in a non-equilibrium state. There are several ways to create a non-equilibrium state. There are several of deuterium atoms within the metal matrix. One is the electrochemical charging, where a D/Pd ratio of ≈ 0.8 can be reached. However, such measurements do not seem to be very reproducible [1,2]. Another possibility is to charge the metal with D to the saturation level from the gas phase at room temperature and then suddenly quench the sample to liquid-nitrogen temperature [14]. One problem in such measurements is that Ti is very reactive and forms a stable surface oxide, which is a barrier to hydrogen uptake. The oxide is decomposed only by annealing to temperatures at 700 °C. A third possibility is to ion-implant the D into, e.g., Pd at low temperatures of the order 25 K. Thereby a supersaturated solution with a D/Pd ratio of 1.3-1.6 is created [15,16]. Myers and coworkers have searched for cold fusion in such systems [16].

In the present study, a fourth possibility, to search for cold fusion in plasma-charged D-Pd and D-Ti, was tried out. A DC glow-discharge was established in a deuterium gas between two water-cooled Cu electrodes, 4 cm apart, in a small reaction cell which is pumped by a normal diffusion pump. The background pressure was 1×10^{-6} torr, and the pressure of the D_2 gas varied between 1 and 5 torr. The Pd and Ti samples, with a surface area of approximately 1 cm^2 , were placed on the cathode, and the DC voltage across the plasma varied between 200 and 400 V. The corresponding current drawn varied between 2-6 mA.

A thin (50 Å) Cu layer was evaporated onto the Pd samples. The heat of solution of D_2 in Cu and Pd is 0.55 eV and -0.18 eV, respectively [9,10], measured relative to the energy level of a D_2 molecule. Thus, by embedding an exothermic metal Pd in a thin layer of Cu, which is highly endothermic to hydrogen uptake, we establish a barrier which prevents/reduces the escape of D from the Pd at least at room temperature.

The impinging deuterium with energies ranging up to 200-400 eV loses approximately 100 eV during the penetration of the Cu layer and thus enters the Pd host with an energy below the threshold for creation of Frenkel pairs. The deuterium ions thermalize very quickly in the Pd host, within the first 50 Å [17]. One could worry that the bombardment of an approximately 100 Å thick surface deuteride could give a detectable neutron yield. However, with a D-D fusion cross section given by:

$$\sigma(E) = (2S(E)/E) \cdot \exp(-\beta/\sqrt{E})$$

where the fusion neutron S-function is 53 keV barn, and $\beta = 44.4021 (\text{keV})^{1/2}$ for energies less than a few keV [18], it can be estimated that for a incident D current of 6 mA and a D ener-

gy of 500 eV, approximately 1.7×10^{-14} neutrons are produced per minute. Such a "surface effect" can thus be neglected. This fact was also tested experimentally by increasing the DC potential over the plasma to 800 V, and no change in the neutron count rate was observed.

Neutrons were detected with an NE213 liquid scintillator (5" diameter and 2" thick), coupled to a fast photomultiplier tube. The pulse-shape discrimination (PSD) technique was employed to distinguish gamma counts from neutron counts, i.e., the difference in zero crossing time of the differentiated pulses was measured. The intrinsic efficiency of the neutron counter was 20% as determined with a calibrated AmBe neutron source, with the threshold set at about 80-100 keV (electron-equivalent), corresponding to neutron energies of 400-500 keV. The neutron counter was placed 5 cm away from the sample in the reaction cell, and the detection efficiency for neutrons in the sample geometry was 3%. Besides the time spectrum, which separates the gamma and neutron counts, a two-dimensional energy-time spectrum was set up, and our interest especially focussed on the region where 2.4 MeV neutrons from the D-D reaction were expected.

The samples were charged with deuterium during the measurements which continued for periods up to two weeks. With a DC current of 6 mA, it takes approximately 8 hours to saturate 1 μm Pd with D. The amount of D in the 1 μm sample was detected by means of the $^3\text{He}(\text{D},\text{p})^4\text{He}$ nuclear reaction [7,19] and found to be $\text{D}/\text{Pd}=0.8 \pm 0.1$.

The background neutron counts were measured by removing the Pd or Ti samples containing the D_2 gas, by removing the D_2 gas

by pumping, and by measuring on a thick (3 mm) Pd crystal so that we had only D in low concentration in solid solution in the Pd crystal. The three different background measurements were internally consistent within the statistical uncertainty. The detected background neutron level was 0.6 n/min, corresponding to a background of 0.3 n/s. The experimental setup was placed two floors below ground level and shielded by 10 cm thick lead bricks.

In Table 1, the experimental results are listed. As can be seen, measurements were carried out on three different Pd samples, an evaporated one, a cold-worked one, and a single crystal, to see whether the defect structure had any influence on the results. Furthermore, one Ti sample, charged from the gas phase to a stoichiometry of $TiD_{1.28}$ prior to the measurements in the reaction cell, was also investigated. As can be seen from the table, no increase in the neutron count rate above the background level was observed. From the measurements in Table 1, an upper limit on the "cold fusion rate" for D+D is found to be $\lambda_f \leq 5 \times 10^{-24}$ fusions/deuteron pair/sec. This is of the same order of magnitude as the value stated by Jones et al [2,3] but significantly lower than that extracted from Pons and Fleischmann's results [1].

In conclusion, we find no evidence for cold fusion from our measurements.

REFERENCES

- 1) M. Fleischmann, S. Pons, J. Electroanalytical Chem 261 (1989) 301 and erratum ibid. 263 (1989) 187
M. Fleischmann, S. Pons and M. Hawkins, erratum, ibid.
- 2) S.E. Jones, E.P. Palmer, J.B. Czirr, D.L. Decker, G.L. Jensen, J.M. Thorne, S.F. Taylor, J. Rafelski, Nature 338 (1989) 737.
- 3) Conference on Cold Fusion, Santa Fe, NM, May 23-25, 1989, Book of Abstracts
- 4) F. Besenbacher, B. Bech Nielsen, S.M. Myers, and J.K. Nørskov, in preparation
- 5) F. Besenbacher, S.M. Myers and J.K. Nørskov, Nucl.Instrum. Methods in Physics Research B7/8 (1985) 55
- 6) P. Nordlander, J.K. Nørskov, F. Besenbacher and S.M. Myers, Phys.Rev.B 40 (1989) 1990
- 7) S.M. Myers, P.M. Richards, W.R. Wampler and F. Besenbacher, J.Nucl.Mater. 165 (1989) 9
- 8) J.K. Nørskov and F. Besenbacher, J.Less.Comm. Metals, 310 (1987) 475
- 9) P. Nordlander, J.K. Nørskov and F. Besenbacher, J.Phys.F: Metal Phys. 16 (1986) 1161
- 10) Hydrogen in Metals Vol 1&2 eds. G. Alefeld and J. Vökl (Springer Verlag, Berlin, 1978)
- 11) O.B. Christensen, P.D. Ditlevsen, K.W. Jacobsen, P. Stoltze, O.H. Nielsen, and J.K. Nørskov, Phys. Rev 40 (1989) 1993
- 12) S.M. Myers, P. Nordlander, F. Besenbacher, and J.K. Nørskov, Phys.Rev.B 33 (1986) 854

- 13) F. Besenbacher, S.M. Myers, P. Nordlander, and J.K. Nørskov,
J.Appl.Phys. 61 (1987) 1788
- 14) A. De Ninno, A. Frattolillo, G. Lollobattista, L. Martinis,
M. Martone, L. Mori, S. Podda and F. Scaramuzzi, Europhysics
Letters 9 (1989) 221
- 15) W. Möller, F. Besenbacher and J. Bøttiger, Appl.Phys A27
(1982) 19
- 16) S.M. Myers, D.M. Follstaedt, J.E. Schriber, and P.M. Ri-
chards, to be published in the Proceedings of the Santa Fe
Workshop on Cold Fusion
- 17) Using the TRIM Code, J.F. Ziegler, J.P. Biersack, and U.
Littmark, *The Stopping and Range of Ions in Solids* (Perga-
mon, New York, 1985)
- 18) N. Jarmie and R.E. Brown, Nucl.Instrum.Methods in Phys.Res.
B10/11 (1985) 405, and private communication
- 19) W. Möller and F. Besenbacher, Nucl.Instrum. Methods 168
(1980)

Table 1

Four different samples were used:

- 1: 1 μm Pd, evaporated, with 50 Å Cu on top
- 2: 25 μm Pd, cold worked, with 50 Å Cu on top
- 3: 1 μm Pd, single crystal, with 50 Å Cu on top
- 4: 1 μm Ti , charged from the gas phase to $\text{TiD}_{1.28}$ prior to submission in the reaction cell.

Measured Count rate

- 1: 0.59 \pm 0.01 n/min
- 2: 0.60 \pm 0.01 n/min
- 3: 0.62 \pm 0.01 n/min
- 4: 0.61 \pm 0.01 n/min
- Background 0.60 \pm 0.01 n/min

THEORY OF HYDROGEN INTERACTION WITH METALS*

J. K. NØRSKOV^a and F. BESENBACHER^b

Haldor Topsøe Research Laboratories, DK-2800 Lyngby (Denmark) and NORDITA, Blegdamsvej 17, DK-2100 Copenhagen (Denmark)

^bUniversity of Århus, Institute of Physics, DK-8000 Århus (Denmark)
(Received May 29, 1986)

Summary

The present understanding of hydrogen interacting with metals as provided by the effective medium theory and self-consistent model calculations is reviewed. An extremely simple picture of the hydrogen-metal interaction is developed capable of describing in a quantitative way a vast number of experimentally observed phenomena such as the molecular adsorption and dissociation process, the properties of chemisorbed hydrogen, surface and bulk diffusion, interstitial hydrogen and the trapping of hydrogen at defects.

1. Introduction

In this paper we will discuss a theoretical picture of hydrogen interacting with metals. It is not the aim to give a review of the field but rather to show that a particular point of view can describe a vast number of experimental observations. We shall be discussing chemisorbed hydrogen, interstitial hydrogen, hydrogen diffusing, and hydrogen interacting with defects and impurities.

Most of the discussion here will be based on the effective medium theory [1] which is a simplified way of calculating total energies for complex, low symmetry systems where ordinary *ab initio* methods are currently not available. The basis for the method is the observation that the total energy is a unique functional of the electron density of the system and that the energy is stationary with respect to variations in the density around the ground state value [2]. This means that an error made in the density will only show up to second order in the calculated total energy. The total energies are therefore simpler to calculate than the electron density or any other property of the system such as the one-electron spectrum.

In a calculation of, for example, the interaction energy of a hydrogen atom with a metal, we can explore this by making a particular ansatz for the

*Paper presented at the International Symposium on the Properties and Applications of Metal Hydrides V, Maubuisson, France, May 25 - 30, 1986.

**INTERACTION OF HYDROGEN ISOTOPES WITH METALS:
DEUTERIUM TRAPPED AT LATTICE DEFECTS IN PALLADIUM**

F. Besenbacher and B. Bech Nielsen
Institute of Physics, University of Aarhus
DK-8000 Aarhus C, Denmark

J.K. Nørskov
Laboratory of Applied Physics, Technical University of Denmark
DK-2800 Lyngby, Denmark

S.M. Myers
Sandia National Laboratories
Albuquerque, NM 87185, USA

P. Nordlander
Dept. of Physics and Astronomy, Rutgers University,
Piscataway, NJ 08855-0849, USA

TEXAS A&M UNIVERSITY

DEPARTMENT OF CHEMISTRY
COLLEGE STATION, TEXAS 77843-3255



August 23, 1989

(409) 845-2011
FAX (409) 845-4719

Dr. William Woodard
U.S. Department of Energy
ER-6 3F-061
Office of Energy Research
100 Independence Avenue, SW
Washington, DC 20077-9381

Dear Dr. Woodard,

In reply to your letter to Dr. Bockris of August 9, 1989, requesting information about our tritium work, Dr. Bockris has asked me to provide the relevant information. In general, almost all of your comments are answered in the enclosed paper which has been accepted for publication in the Journal of Electroanalytical and Interfacial Electrochemistry. However, there are a few points which I will answer here:

- Point 5d By PhD_n , I assume you are referring to the Pd/D ratio in the cells that produced ^3H . This investigation was not performed.
- Point 6 (Neutron production) Please refer to Dr. Kevin Wolf's report for this information.
- Point 7 (Heat production) Due to the size of the electrodes (in general 1mm x 4cm), the amount of heat produced concomitant with the tritium would not have been able to have been detected in our present calorimeters. Therefore, none of the cells in which tritium is reported were ever put into a calorimeter.
- Point 8 (Tritium Sources) There is a small supply of tritiated water present in our laboratories in a room 2 floors above the labs in which our cells were running. There was also a positive result in the Cyclotron Institute in which there is no tritium supply.

I think this should answer most of your questions, but if there are any others, please do not hesitate to contact me on (409) 845-0909.

Sincerely,

Nigel J.C. Packham

cc: Prof. J. Bigeleisen

PRODUCTION OF TRITIUM FROM D_2O ELECTROLYSIS
AT A PALLADIUM CATHODE

N.J.C. Packham, K.L. Wolf, J.C. Wass, R.C. Kainthla and J.O'M. Bockris
Department of Chemistry and the Cyclotron Institute, Texas A&M University
College Station, Texas 77843

PRODUCTION OF TRITIUM FROM D₂O ELECTROLYSIS
AT A PALLADIUM CATHODE

N.J.C. Packham, K.L. Wolf, J.C. Wass, R.C. Kainthla and J.O'M. Bockris
Department of Chemistry and the Cyclotron Institute, Texas A&M University
College Station, Texas 77843

INTRODUCTION

In the present communication, we report data that may be relevant to the phenomenon of room temperature fusion [1]. It is the contention of the authors that the alleged phenomenon is better characterized by the production of nuclear particles than by the measurement of bursts of heat. Here, we describe the observation of tritium produced in eleven D₂O electrolysis cells at levels 10²-10⁵ times above that expected from the normal isotopic enrichment of electrolysis. Particular attention has been paid to possible sources of contamination.

EXPERIMENTAL

Pd cathodes of diameters 1 to 6mm were subjected to D₂ evolution from D₂O-0.1M LiOD electrolysis. The resulting solutions and the gases were examined for tritium.

Samples of liquid electrolyte were measured using liquid scintillation counting.

In all cells, measurements were made for the activity of ³H in solution, and in one cell, gases evolved were recombined external to the cell using 0.5% platinum on alumina catalytic beads (recombination catalyst). The resulting liquid was analyzed in the same way as the electrolyte samples.

Twenty four electrochemical cells were fabricated using 15 ml Pyrex centrifuge tubes. The ends of the tubes were sealed with Viton rubber septa, through which electrode connections were made. Palladium samples supplied by

Hoover and Strong (Richmond, VA), via the Texas Coin Exchange, 1 mm by 4 cm, and 3mm by 4 cm in dimension (99.9% purity) were prepared as shown in Table 1. 6mm x 4cm electrodes were obtained from SurePure Chemetals Inc. All electrode connections were made using 99.9% pure nickel wire (0.5 mm), spot welded to the palladium wires. The nickel connections were fed through the septa, to form an air-tight seal. Nickel gauze anodes (99.9% pure) used in all cases, were washed in 5N HCl, then in D₂O, and allowed to air dry. A 0.1M LiOD solution was prepared using 99.9% pure lithium metal from Alfa associates, which was added to 1 liter of 99.9% pure deuterium oxide (Aldrich Chemical Co.), in an atmospheric bag containing argon. Additions to the cells (D₂O, LiOD refilling) were made through the rubber septum using disposable syringes (one use only), equipped with stainless steel needles. Gases evolved during electrolysis were allowed to escape through a needle, pierced through the septum, attached via Tygon tubing to a mineral oil bath to avoid light water contamination. In general, the 1mm cells were at first run galvanostatically at 60 mAcm⁻² for 14 to 16 days, the 3mm electrodes being charged for up to 28 days. Throughout this period, additions of D₂O were made (1 to 2 ml per day at low current density and up to 3 to 4 ml per hour at high current density). The potential and current density through each cell was monitored 24 hours a day. After the time stated, the current density was increased to 500 mAcm⁻² for periods up to 12 hours. Samples of electrolyte were withdrawn for tritium analysis from the cell using a sterile syringe (later discarded).

Tritium analysis was performed on the alkaline electrolyte by in-situ Liquid Scintillation Counting (LSC). Three counters were used in these analyses. The first of these is a Wallac LKB model 1219 LSC; the second, a Wallac LKB model 1410, and the third an instrument constructed in the

Cyclotron Institute. A water soluble scintillation cocktail (Biosafe II, Research Products International Corporation, 15 ml) was added to 1 ml of sample, and allowed to stand under cover for 30 minutes before counting, which was found to be sufficient for elimination of chemiluminescence contributions for the work reported here. The samples were then analyzed in a double-blind fashion (with respect to the operator of the counter). Multiple blank samples of H_2O , D_2O , and 0.1M LiOD were included for analysis. Evidence for chemiluminescence of the scintillation cocktail had been discovered when samples of 1M LiOD had been analyzed. Therefore, a test was made using samples ranging from 1M to 0.01M LiOD, and including samples that had been neutralized by potassium hydrogen phthalate (KHP). Results of these experiments are shown in Fig.1, which set the criterion for eradication of chemiluminescence. Samples run 24 hours later, show no significant change in activity levels. The efficiency of the model 1219 detector for tritium in the samples was 33%, for the model 1410 around 40%, and for the counter constructed in the Cyclotron Institute, around 30%. One minute and ten minute analyses (some samples were run overnight) were performed. A detailed analysis of the energy spectra from the Cyclotron Institute counters yielded the correct β energy end point for tritium (18keV). The results are given as counts per minute (cpm) per ml of sample, and as disintegrations per minute (dpm) per ml of samples. The conversion factor is given by:

$$dpmml^{-1} = (cpmml^{-1} \text{ sample} - cpm \text{ cocktail}) \times (V/E),$$

where E is the efficiency of the detector and V is the volume factor to give results per ml of sample.

After the analysis at Texas A&M, an examination of the tritium content of liquids resulting from the electrolysis, including a tritium (HTO) standard

and blanks of LiOD and D₂O, was made by Los Alamos National Laboratory (National Tritium Center), Argonne National Laboratory, Battelle Pacific Northwest Laboratory and at the General Motors Research Laboratory. These results are shown in Table 2.

One of the cells used in the experiment (cell A8) also featured an external gas recombination arrangement using 0.5% platinum on alumina pellets which gave close to 100% recombination at low current densities (50 mAcm⁻²).

The tritium production of this cell was followed for a further period of time. It had been charged at low current density (50 mAcm⁻²) for 16 days, and then put to 500 mAcm⁻² for 8 hours, after which, it was returned to the charging current, since the levels of tritium were at background. After 4 weeks, the recombination catalyst was put in place, and the recombinant was collected for 2 weeks. After this, the activity in the recombined gas and the electrolyte was measured on the 1410 LSC, resulting in the highest level found in all 9 cells. These results are shown in Table 3b.

Another cell (cell A2) was tested for tritium over an extended period of time. It was initially run at low current density for 16 days, followed by a 10 hour period at high current density, after which, tritium was not produced. The cell was then transferred to the Cyclotron Institute where it remained at low current density for another week, with no tritium production. On May 6, the current was increased to 110 mAcm⁻² for two hours, increased again to 300 mAcm⁻² for 20 minutes, decreased to 90 mAcm⁻² for seven days at which point it was returned to 50 mAcm⁻² until June 22. The tritium content of the solution was monitored during this time and the results are shown in Fig. 2, which limits the apparent production period to approximately 2 days.

In one of the cells (cell A7) the build up of tritium as a function of

time was followed in more detail at high current density. The results shown in Fig. 3. place a limit on a period of production of approximately 12 hours.

The possibility that tritium was present in the D_2O , and the Li is ruled out by the results of Tables 3a and 3b. Each batch of D_2O that was used for refilling the cells was analyzed for tritium content, both on the 1219 instrument (Table 3a), and the 1410 (Table 3b, shown as a mean of 10 results). Several experiments were run in which no tritium was observed., including identical cells to the ones which did produce tritium, except for the electrolyte, which was 0.1M LiOH in H_2O (Tables 3b and 4). Possible contamination from the nickel anode was examined by dissolving an unused piece of nickel from the same large sheet used for all counter electrodes in concentrated nitric acid, followed by neutralization and then counting, with negative results.

Samples of virgin palladium and nickel of the same batch used for all 1mm Pd cells were sent for analysis to Los Alamos National Laboratory. Thermal desorption mass spectrometry was used and no tritium was found in either electrode material (and likewise use for the last 4 entries in Table 4., i.e. D_2O and H_2O blanks). In addition, palladium is used throughout as a cathode, the electrochemical nature of which would tend to drive H (D,T) into the cathode, rather than evolve tritium from within the electrode.

Interference with the experiments is considered improbable because of positive results from the Cyclotron Institute to which entrance is prohibited except by the usual personnel at the Institute. There are also no supplies of tritium at the Cyclotron. In advertent contamination is unlikely because no tritium work has been performed in either of the laboratories involved.

RESULTS

The results and noteworthy features of the cells are summarized in Tables 1, 2, 3 and 4, some features of which are listed below.

1) Electrodes produced tritium in different time domains (i.e. cell A2 and A8), of which some electrodes required lengthy low current density treatment (up to 9 weeks) before production.

2) Ni gauze (NiO_2) was the anode material in all experiments reported here, in contrast to platinum wire or gauze used by most investigators.

3) The tritium concentration in solution (DT?) increases with time until it reaches an asymptote (Fig. 3), which can be interpreted in terms of the end point of production. Tritium production at the electrode ceases after some hours of activity (Figs. 2 and 3)

4) Tritium from the D_2 -DT mixtures evolved from the electrode gives rise, after recombination, to a solution concentration about 100 times greater than that with which the gas off from the electrode is in equilibrium.

DISCUSSION

It can be shown that¹ prolonged electrolysis of a solution regularly make up to constant volume by addition of D_2O gives an isotope enrichment equal to the known separation factor of H,D,T, i.e. at a negligible level compared to the results reported in Table 1 for the 9 most active cells.

Reports of tritium production can always be questioned as to contamination. Defence against each suspicion has to be made each time a new suspicion is expressed. Tables 3 & 4 show that an extensive program of checks and blanks has been performed.

The electrode surface seems to be involved in the nuclear events implied

¹G. Lin and J. O'M. Bockris, developing a communication from M. Fleischmann

here since, according to Storms [2], a tritium producing Pd cathode, when made anodic in a virgin D_2O -LiOD solution, produced no tritium, i.e. none dissolved from inside the electrode.

In further support of the present observations, several others have been made [2-5].

We are aware that, according to the classical theory of nuclear physics, when D-D fusion occurs, the rate of neutron production should be approximately equal to that of tritium. This is not observed in the present experimental program [6]. We believe that it is important firstly to establish the facts about tritium production on electrodes. The theory of electrochemical confinement will be discussed elsewhere.

ACKNOWLEDGEMENT

We are grateful to the Welch Foundation, Texas A&M University and the Electric Power Research Institute for financial support, to our colleagues in the Surface Electrochemistry Laboratory for numerous helpful acts during the experimental work, and to the Health Physics Department at Texas A&M University for their frequent and thorough (negative) searches for contamination of the laboratories and personnel.

TABLE 1
CELL IDENTIFICATION, ELECTRODE TREATMENT, SOLUTION TYPE AND TRITIUM ACTIVITY
OF ELECTROLYTE SAMPLES PERFORMED ON 1219 LSC

CELL	ELECTRODE PRETREATMENT ^a	SOLUTION	CORRECTED ³ H ACTIVITY (dpmml ⁻¹)
A1	No treatment	0.1M LiOD	3.8 x 10 ⁴
A2	No treatment	0.1M LiOD + 0.1mM NaCN	
	After 16 days at 50 mAcm ⁻² then		
	for 8 hours at 500 mAcm ⁻² (5/1/89)		168
	50 mAcm ⁻² for 4 days (5/5/89)		134
	50 mAcm ⁻² for 3 hours, 110 mAcm ⁻² for		
	2 hours, 200 mAcm ⁻² for 20 minutes (5/6/89)		1.1 x 10 ⁴
	50 mAcm ⁻² (5/7/89)		1.4 x 10 ⁴
	(5/7/89 - 5/13/89)		1.1 x 10 ⁴
	(5/13/89 - 6/6/89)		7.5 x 10 ³
A3	Anneal	0.1M LiOD	4.9 x 10 ⁶
A4	Anneal	0.1M LiOD + 0.1mM NaCN	1.2 x 10 ⁵
A5	Acid Etch	0.1M LiOD	3.7 x 10 ⁶
A6	Acid Etch	0.1M LiOD + 0.1mM NaCN	3.3 x 10 ⁴
A7	Electrochemical	0.1M LiOD	
	Before high current density		102
	After 2 hours at 500 mAcm ⁻²		5223
	After 6 hours at 500 mAcm ⁻²		5.0 x 10 ⁵
	After 12 hours at 500 mAcm ⁻²		7.6 x 10 ⁵
A8	Electrochemical	0.1M LiOD + 0.1mM NaCN	
	After 16 days charging and 8 hours		192
	high current density (5/1/89)		
	Electrolyte levels after 6 weeks		5.0 x 10 ⁵
	at 50 mAcm ⁻²		
	Recombined gas levels after 2 weeks		
	of external recombination at 50 mAcm ⁻²		5.0 x 10 ⁷
B3 (3mm)	Anneal	0.1M LiOD	6.3 x 10 ⁴
B5 (3mm)	Acid Etch	0.1M LiOD	48
CELL 1 (6mm)	No treatment	0.1M LiOD	117

^a Key for electrode surface pre-treatment: Anneal = annealing at 800 °C, 10⁻⁶ torr, 8 hours; Acid etch in 5M HCl, 15 minutes; Electrochemical oxide removal, 2 hours

TABLE 2

CONFIRMATORY RESULTS FROM OUTSIDE SOURCES ON VARIOUS SAMPLES
CORRECTED ^3H ACTIVITY IN dpmml^{-1}

SAMPLE	CELL 1*	CELL 2*	HTO STANDARD	0.1M LiOD	D ₂ O
INSTITUTION					
Texas A&M	2.13×10^6	1157	7.23×10^5	93	47
Battelle	1.96×10^6	1170	8.08×10^5	127	140
Argonne	1.96×10^6	1020	7.59×10^5	90	114
Los Alamos	1.97×10^6	800-1300	6.50×10^5	113	161
General Motors	1.80×10^6	1000	-----NOT ANALYZED-----		

*Cell 1 corresponds to cell A1 in Table 1 approximately 1 week after the high current density treatment, whereas, cell 2 corresponds to cell A5 in Table 1 before high current density treatment.

$2 \times 10^6 \neq 4 \times 10^4$
 $10^3 \neq 4 \times 10^1$

TABLE 3a

BLANK EXPERIMENTS DURING TRITIUM ANALYSIS
PERFORMED ON THE 1219 COUNTER

SAMPLE	cpmm ⁻¹	BACKGROUND CORRECTED ACTIVITY (dpmml ⁻¹)
D ₂ O Analysis #1	65	48
D ₂ O Analysis #2	70	63
D ₂ O Analysis #3	67	54
D ₂ O Analysis #4	60	33
D ₂ O Analysis #5	50	3
D ₂ O Analysis #6	71	66
D ₂ O Analysis #7	75	78
D ₂ O Analysis #8	62	39
0.1M LiOD Analysis #1	75	78
0.1M LiOD Analysis #2	70	63
0.1M LiOD Analysis #3	74	75
0.1M LiOD Analysis #4	65	48
0.1M LiOD Analysis #5	60	33
0.1M LiOD Analysis #6	66	51
0.1M LiOD Analysis #7	76	81
0.1M LiOD Analysis #8	70	63
Neutralized 0.1M LiOD	73	72
Neutralized 0.1M LiOD + 0.1mM NaCN	76	81
Dissolved nickel in acid Analysis #1	78	87
Dissolved nickel in acid Analysis #2	80	93
Dissolved nickel in acid Analysis #3	76	81
Scintillation cocktail	49	--

TABLE 3b

MEAN OF 10 BLANK EXPERIMENTS DURING TRITIUM ANALYSIS
PERFORMED ON THE 1410 COUNTER

SAMPLE	cpmm1 ⁻¹	BACKGROUND CORRECTED ACTIVITY (dpmm1 ⁻¹)
BIOSAFE II COCKTAIL	170±13	---
H ₂ O Analysis	161±16	0
D ₂ O Analysis	210±16	100
0.1M LiOD Analysis	220±20	125
0.1M LiOH Analysis	157±12	0
Dissolved Nickel in Nitric Acid	140±20	0
Tygon Tubing in NaOH	105±20	0
Rubber Stoppers in NaOH	150±20	0
Recombination Catalyst in NaOH	140±15	0
Dissolved Shavings from Cutters	160±11	0
Dissolved Shavings from Vacuum Chamber	164±17	0
Dissolved Shavings from Spotwelder	155±10	0

TABLE 4
 DETAILS OF CELLS THAT PRODUCED NO TRITIUM
 WITH 1410 LSC (CORRECTED ACTIVITY)

EXPERIMENT	dpmm ⁻¹
3mm x 3cm Ti Cathode in 0.1M LiOD with internal gas recombination	275
3mm x 3cm Pd Cathode in 0.1M LiOD with internal gas recombination	235
3mm x 3cm Ti Cathode in 0.1M LiOD with internal gas recombination	285
0.5mm x 1cm Pd Cathode in 0.1M LiOD with internal gas recombination	55
4mm x 2mm Pd disc Cathode in 0.1M LiOD with internal gas recombination	365
0.5mm x 1cm Pd Cathode in 0.1M LiOD with external gas recombination (recombined gases measured)	315
1mm x 4cm Pd Cathode in 0.1M LiOD with external gas recombination (recombined gases measured 7/18/89)	75
1mm x 4cm Pd Cathode in 0.1M LiOD with external gas recombination (recombined gases measured 7/21/89)	33
1mm x 4cm Pd Cathode in 0.1M LiOH (H ₂ O) No gas recombination	0
1mm x 4cm Pd Cathode in 0.1M LiOH (H ₂ O) No gas recombination	18

REFERENCES

- 1) M. Fleischmann and S. Pons, J. Electroanal. Chem., 261 (1989) 301.
- 2) E. Storms, Private Communication, July 1989.
- 3) G.J. Schoessow and J.A. Wethington, Private Communication, July 1989.
- 4) P. Ramirez, Private Communication, July 1989.
- 5) R. Adzic, Private Communication, July 1989.
- 6) K.L. Wolf, N.J.C. Packham, D. Lawson, J. Shoemaker, F. Cheng and J.C. Wass., Proceedings of the Workshop on Cold Fusion Phenomena, Santa Fe, NM., May 1989,

New Energy Times Archive

FIGURE CAPTIONS

Figure 1. The effect of electrolyte concentration on chemiluminescence of the scintillation cocktail.

Figure 2. The production of tritium in the electrolyte of cell A2 as a function of time (ordinate gives date).

Figure 3. The production of tritium in the electrolyte of cell A7 as a function of time.

New Energy Times Archive

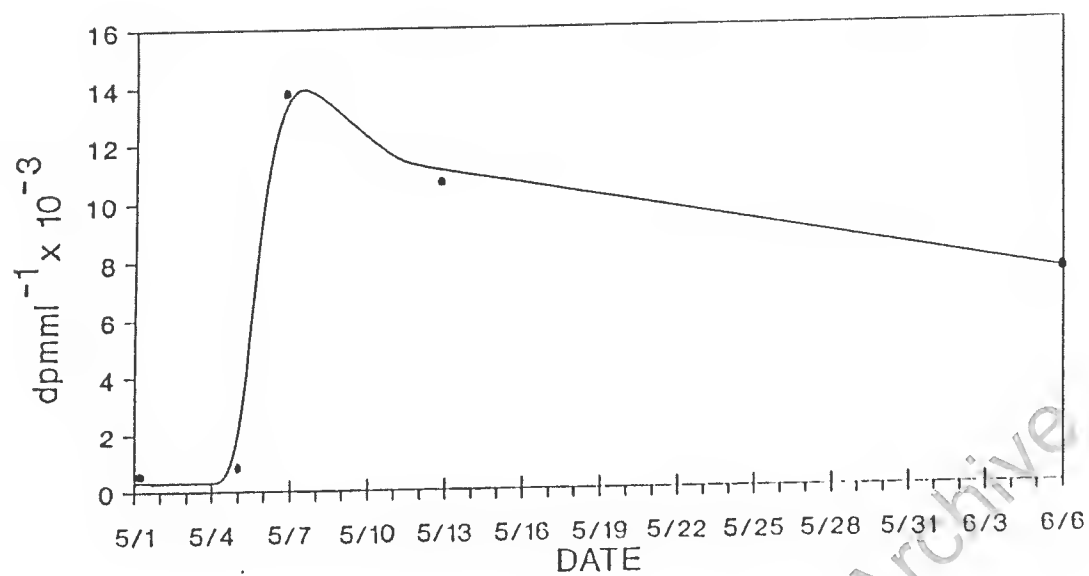


FIG 2.

TIME PROFILE OF TRITIUM PRODUCTION FROM CELL A7

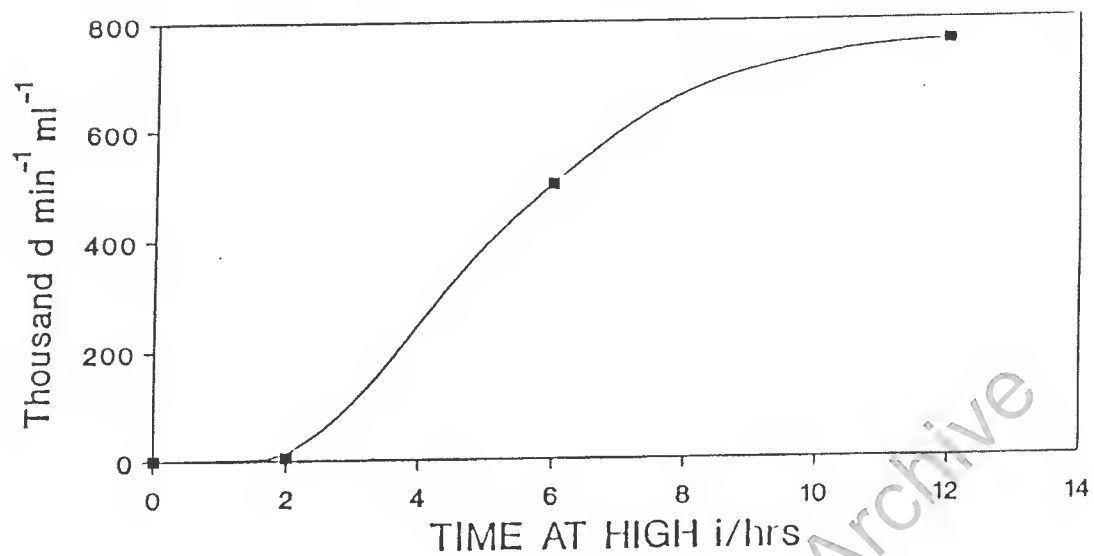


FIG. 3

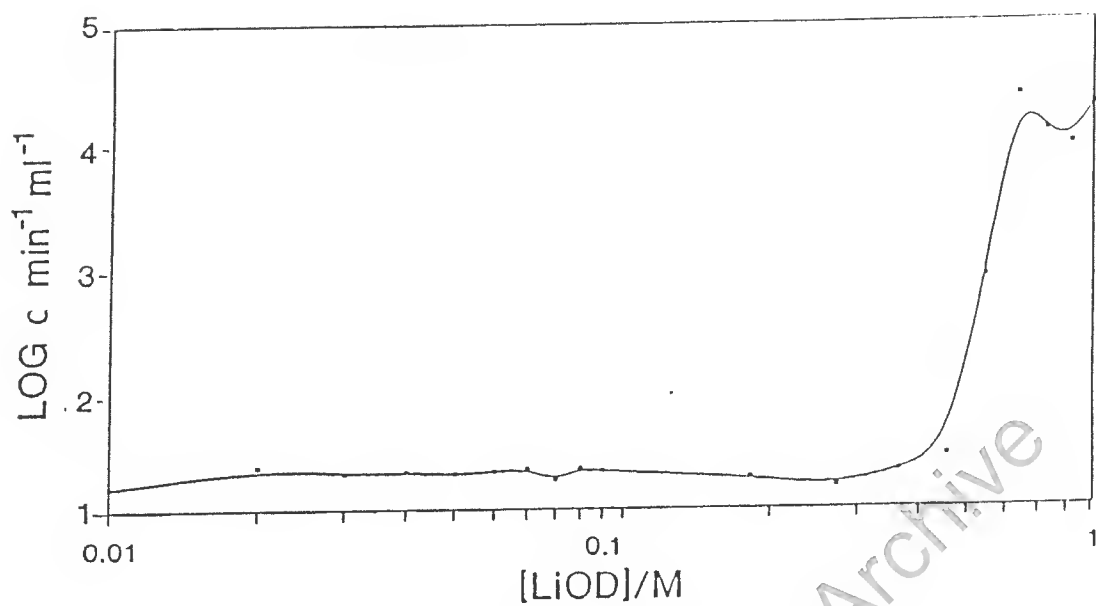


FIG 1

1989 AUG 4

Submitted to Journal of Fusion Energy as part of the Proceedings of the Workshop
on Cold Fusion Phenomena held in Santa Fe in 1989 May.

IN SEARCH OF NUCLEAR FUSION IN ELECTROLYTIC CELLS
AND IN METAL/GAS SYSTEMS

D.R. McCracken, J. Paquette, H.A. Boniface, W.R.C. Graham,
R.E. Johnson, N.A. Briden, W.G. Cross, A. Arneja,
D.C. Tennant, M.A. Lone and W.J.L. Buyers

Atomic Energy of Canada Limited
Chalk River Nuclear Laboratories
Chalk River, Ontario, Canada K0J 1J0

and

K.W. Chambers, A.K. McIlwain, E.M. Attas and R. Dutton

Atomic Energy of Canada Limited
Whiteshell Nuclear Research Establishment
Pinawa, Manitoba, Canada R0E 1L0

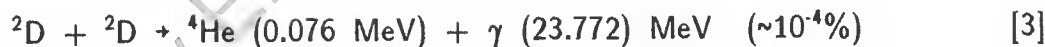
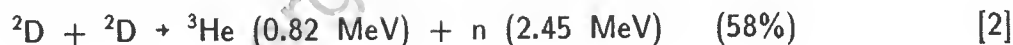
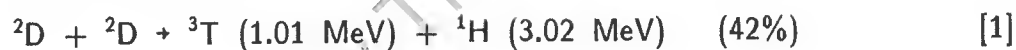
ABSTRACT

It has been reported recently in the literature that unexpected thermal and nuclear effects (production of excess heat, neutrons, γ -rays, and tritium) can occur during the electrolysis of heavy water at palladium or titanium electrodes, or during temperature and pressure cycling of the titanium/deuterium gas system. We have attempted to reproduce some of these experiments. A variety of electrochemical cells having palladium cathodes in the form of wires, tubes, sheets and rods have been used to electrolyse heavy water containing $0.1 \text{ mol.dm}^{-3} \text{ LiOH}$, $0.1 \text{ mol.dm}^{-3} \text{ LiOD}$ or $0.5 \text{ mol.dm}^{-3} \text{ D}_3\text{PO}_4$. Current densities of up to 200 mA.cm^{-2} were applied. The mass of the palladium cathodes covered the range from 1 to 40 grams and the surface area varied from 8 to 140 cm^2 . Neutron detection systems with low constant backgrounds were used to search for neutron emission during electrolysis. These included ^3He - and $^{10}\text{BF}_3$ -based detectors. After running some of the cells for more than 30 days, no neutron emission above background could be detected. This puts upper limits of 0.5 s^{-1} and $2 \times 10^{-23} \text{ fus.D-D.s}^{-1}$ on the neutron emission and the fusion rate, respectively. A sensitive and accurate heat-flow calorimeter was built and used to monitor the energy balance of some of the cells during electrolysis. No unexpected heat effects were observed. This puts an upper limit of 0.13 W.cm^{-3} on the specific excess power. No enrichment of the electrolyte in tritium was evident after electrolysis. Experiments were also performed with the titanium/deuterium gas system. These consisted of exposing titanium metal to a deuterium gas pressure of 40 atmospheres, lowering the temperature to -196°C , releasing the pressure and gradually warming the titanium to room temperature. No neutron emission above background was observed during these experiments, which puts upper limits of 0.5 s^{-1} and $4 \times 10^{-25} \text{ fus.D-D.s}^{-1}$ on the neutron emission and fusion rate, respectively.

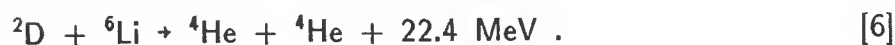
INTRODUCTION

Three papers have appeared recently that report the occurrence of unexpected thermal and nuclear effects (i.e., production of excess heat, neutrons, γ -rays and tritium) during the electrolysis of heavy water at palladium or titanium electrodes at room temperature and atmospheric pressure⁽¹⁻³⁾. These effects were attributed to nuclear fusion of deuterium at, or in, the palladium or titanium electrodes. The emission of bursts of neutrons has been reported recently for the system titanium/deuterium gas following pressure and temperature cycling and has also been attributed to fusion of deuterium⁽⁴⁾. We have attempted to duplicate some of these experiments.

Nuclear fusion of deuterium should result in the production of heat, neutrons, γ -rays, tritium and helium through nuclear reactions such as



The following reactions could also occur, if hydrogen and lithium are present:



Here n signifies neutron, γ stands for γ -ray and the percentages are the branching fractions measured for nuclei screened by muons⁽⁵⁾; the branching factors

should not be much different for nuclei screened by electrons. The rates of reactions [1] and [2] are thus approximately equal, whereas reaction [3] has a much lower rate, even at low energies⁽⁶⁾. Reaction [4] describes the final interaction between fast neutrons and hydrogenated materials. Theoretical calculations⁽⁷⁻⁹⁾ show that reaction [5] could be an important pathway for nuclear fusion at low energies if hydrogen is present, the estimated rate being of the same order of magnitude as that of reactions [1] and [2], if a hypothetical enhancement of the electron mass by a factor >5 is considered. Reaction [6] is expected to be insignificant at low energies since Coulomb repulsion is large, as is the internuclear separation⁽¹⁰⁾.

Because heat can be produced by a variety of chemical and metallurgical phenomena, our experiments have initially focussed on the detection of neutrons, γ -rays and tritium as evidence of nuclear fusion in electrolytic cells, and in the detection of neutrons in the titanium/deuterium gas system. Later on, a calorimeter was built and used to measure the energy balance in electrolytic cells. No evidence of nuclear or unanticipated heat effects was obtained in any of our experiments. Because many of the parameters that could be important in producing the previously reported nuclear and heat effects are not yet known, we describe our experimental procedures in more detail than is customary.

EXPERIMENTAL

Electrochemistry

The electrochemical experiments consisted in electrolysing 0.1 mol.dm^{-3} solutions of LiOH or LiOD in D_2O at various current densities, using palladium cathodes and platinum anodes. The LiOH or LiOD solutions were prepared by dissolving lithium hydroxide, lithium oxide or lithium metal in 99.97% or 99.99% D_2O . In one instance, a $0.5 \text{ mol.dm}^{-3} \text{ D}_3\text{PO}_4/\text{D}_2\text{O}$ solution, obtained by dissolving P_2O_5 in 99.99% D_2O , was used as the electrolyte. The initial tritium content of the

99.97% D_2O was $14.7 \pm 0.1 \text{ Bq.cm}^{-3}$ whereas the initial tritium content of the 99.99% D_2O was $2.43 \pm 0.06 \text{ Bq.cm}^{-3}$, as determined by liquid scintillation counting. For comparison, distilled H_2O was found to contain tritium at a level of $0.47 \pm 0.01 \text{ Bq.cm}^{-3}$. Various constant-current sources were used to perform the electrolysis, including regulated power supplies, a model 173 potentiostat from Princeton Applied Research operating in galvanostat mode and a lead/acid automotive battery (12 Volts) with an automotive battery charger and a ballast resistor. The currents and voltages were measured with digital multimeters. The experiments were performed with a variety of palladium cathodes and electrochemical cells as described below.

Electrochemical cells made of borosilicate glass or quartz and having palladium cathodes in the form of wires, tubes, sheets and rods were used. Current densities of up to 200 mA.cm^{-2} were applied. The mass of the palladium cathodes covered the range from 1 to 40 grams and the surface area varied from 8 to 140 cm^2 . Electrolysis time ranged from 0.5 to more than 30 days. The temperature ranged from 16 to 50°C . Some of the cathodes were subjected to chemical analyses before electrolysis; impurities levels ranged from 3 atom % silver for a commercial palladium/silver alloy to ppm amounts of silver and silicon for a sample of high purity palladium sponge. Various cathode surface preparation techniques were used including abrasion, electropolishing, etching in acid solutions and simple cleaning with solvents. Some of the cathodes were arc-melted, cast, annealed and cold-worked. Others were used as received from the supplier (Johnson Matthey, 99.95%). An interesting aspect of some of the cells (cells 3-5) is the use of a wetproofed catalyst contained in a water-cooled condenser above the aqueous phase. The catalyst, developed by Atomic Energy of Canada Limited, can recombine D_2 and O_2 with high efficiency at low temperature even in the presence of moisture⁽¹¹⁾. This arrangement offers many advantages; evaporative losses of D_2O are eliminated, electrolytic enrichment of tritium is also eliminated and calorimetric measurements are simplified, as discussed later. Table I summarizes the electrochemical parameters for the various cells whereas Table II lists the chemical characteristics of the electrodes and electrolytes. Figure 1 is a schematic representation of a typical electrolytic cell.

A current density of 20 mA.cm^{-2} (requiring 5 V) was applied to the cathode of cell 1 for four days. About 70% of the surface area of the cathode was submerged. The current density was then increased to 70 mA.cm^{-2} (at 6 V) for three additional days. The cathode was then transferred to cell 2, where it was subjected to current densities ranging from 80 to 200 mA.cm^{-2} over a period of more than 30 days. A current density of 80 mA.cm^{-2} was applied to the rod and sheet cathodes of cell 2 for a total of seven days after which the experiment was terminated. Due to the design of that cell, only 60% of the surface area of the cathodes were submerged. A current density of 106 mA.cm^{-2} (6 V) was applied to the rod cathode of cell 3 for five days; the cathode was completely submerged. The electrode was removed from cell 3, abraded with 600-grit silicon carbide paper and transferred to cell 4 where it was subjected to current densities ranging from 100 to 170 mA.cm^{-2} (6.6 V) for 26 days while being completely submerged. Current densities of 53 to 180 mA.cm^{-2} (6.4 V) were applied to the cathode in cell 5 for a period of 45 days. The cathode was completely submerged and the cell was purged continuously with deuterium gas. Cell 6 has been electrolysed at a current density of 70 to 100 mA.cm^{-2} for 28 days. The cathode was completely submerged. Cell 7 was subjected to a current density of 100 mA.cm^{-2} for a period of about 24 hours. Cell 8 was subjected to a current density of 80 to 90 mA.cm^{-2} for a period of 12 hours whereas cells 9 and 10 were electrolysed at a current density of 64 mA.cm^{-2} for a period of 12 hours. Cell 11 was electrolysed at a current density of 100 mA.cm^{-2} for 60 hours. The cathodes in cells 7-11 were completely submerged. Except for the sheet cathode in cell 3, all of the palladium cathodes turned dull grey after a few hours of electrolysis and mottled black on the bottom part of the electrodes after a few days. The test matrix, i.e. which cell was used in what neutron detector for how long, can be inferred from Table IV.

Neutron Detection

Neutron detection was performed with moderated systems using ^3He or $^{10}\text{BF}_3$ detectors. The systems were shielded from external neutrons with cadmium

and wax, plastic, concrete or light water. Moderation was accomplished with wax or plastic. The various neutron detection systems are described in Table III. Neutron detector CRNL 3 was the most extensively used. This detection system, which is illustrated in Figure 2, contains five ^3He detectors selected for their low background. The background summed over all five detectors, as measured with unpowered cells, is low and constant at $(8.3 \pm 0.4) \times 10^{-3} \text{ s}^{-1}$. The efficiency of the detector was determined using Pu/Li, Pu/Be and ^{252}Cf neutron sources having neutron emissions of the order of 10^4 to 10^5 s^{-1} . The sources were placed in the center of quartz tubes of the same geometry and size as for cells 4 and 5 and containing the same amount of water or heavy water as the electrolytic cells so that moderation by water could be taken into account. The overall detector efficiency for 2.5-MeV neutrons was found to be $1.6 \pm 0.8\%$. Except for detector CRNL 4, the efficiencies of the other detectors were estimated. The test matrix, i.e. which electrolytic cell was used in what neutron detector and for how long, can be inferred from Table IV.

A 7.5x7.5-cm sodium iodide scintillation detector was used to monitor for the 2.22-MeV neutron capture γ -rays (reaction [4]) from the wax moderator during the experiments with cell 1. The overall efficiency of the detector for these 2.22-MeV γ -rays, including solid angle, is estimated at 0.1% or less, much lower than the efficiency of the other neutron detection systems.

Calorimetry

Crude calorimetric measurements could be performed with cells 3-5, 10 and 11 by measuring the temperature of the cooling water at the inlet and outlet of the cooling jacket surrounding the cells. If the flow of cooling water to the cell jacket is adjusted so that the temperature of the cell is constant, the power output of the cell, P_{out} , is given by

$$P_{\text{out}} = f \Delta T \cdot C_p \quad [7]$$

where f is the flow rate in g.s^{-1} , ΔT is the temperature difference between the outlet and the inlet in $^{\circ}\text{C}$ and C_p is the heat capacity of water in $\text{J.g}^{-1}.\text{^{\circ}C}^{-1}$. The power input to the cell, P_{in} is given by:

$$P_{\text{in}} = V \cdot I \quad [8]$$

where V is the applied potential in Volts and I is the cell current in Amperes. For a typical flow rate of 10 g.s^{-1} , the minimum detectable excess power ($P_{\text{out}} - P_{\text{in}}$) was about one Watt. For comparison, the excess power ("excess rate of heating") reported by Fleischmann *et al.*⁽¹⁾ for a large rod electrode ($0.4 \times 10 \text{ cm}$) is 1.75 Watts.

A more sensitive and accurate heat-flow calorimeter was built and is illustrated in Figure 4. The calorimeter consists of a submersible glass cell containing the electrolyte, electrodes and wetproofed catalyst, an insulated vacuum bottle containing the cell and a water circulating system. The whole system is kept in a temperature-controlled environment. Water from a reservoir maintained at a constant temperature flows at a known flow rate through a copper coil surrounding the cell which is itself submerged in water in an insulated vacuum bottle. The average flow rate is determined by measuring the weight of the circulated water as a function of time. Thermocouples are used to measure the temperature of the water in the coil at the inlet and outlet of the vacuum bottle as well as the temperature of the water surrounding the cell. The power output (in Watts) of the cell is given by equation [7] whereas the power input is given by equation [8]. The data, including the applied voltage and current, were collected with a microcomputer-based data acquisition system.

Since all of the evolved gases (D_2 and O_2) are recombined inside the calorimeter with an efficiency of 100%, the cell is a closed system with no mass transfer to the outside taking place. This simplifies energy balance calculations because the power used to electrolyse heavy water does not have to be taken into account and no water vapor escapes from the cell. The calorimeter was tested and

calibrated using resistance heaters. The relative accuracy of the instrument is better than 1% of the power input for typical powers of 5 to 20 W. The heat-loss coefficient was found to be $0.35 \text{ W} \cdot ^\circ\text{C}^{-1}$ for temperatures of about 30°C . Because the entire energy output of the cell is measured, the calorimeter is not sensitive to thermal gradients and no stirring of the electrolyte is required. The thermal response time of the system is about one hour.

The cathode rod from cell 2 was cut down to a length of 4 cm giving a palladium rod of dimensions $4.0 \times 0.7 \text{ cm}$. The cathode was used to electrolyse a $0.1 \text{ mol} \cdot \text{dm}^{-3}$ $\text{LiOD}/\text{D}_2\text{O}$ solution in the calorimeter at current densities ranging from 150 to $300 \text{ mA} \cdot \text{cm}^{-2}$, requiring a power input of 5 to 20 Watts. After 27 days of electrolysis time, the electrolyte was made $5 \times 10^{-3} \text{ mol} \cdot \text{dm}^{-3}$ in As_2O_3 to inhibit the recombination of atomic hydrogen on the electrode surface (recombination poisoning). The electrolysis was continued for 20 additional days at a typical current density of $500 \text{ mA} \cdot \text{cm}^{-2}$ requiring a power input of 30 Watts.

A $4.5 \times 0.6\text{-cm}$ palladium rod obtained from Johnson Matthey with a stated purity of 99.95% was used to electrolyse a $0.1 \text{ mol} \cdot \text{dm}^{-3}$ $\text{LiOD}/\text{D}_2\text{O}$ solution at a typical current density of $150 \text{ mA} \cdot \text{cm}^{-2}$ requiring a power input of 15 Watts. The electrolysis lasted for 18 days.

Deuterium Loading

The deuterium content of some of the palladium cathodes was measured after electrolysis using a thermal desorption technique. These analyses were performed by ramping the temperature of a weighed portion of palladium cathode from 20 to 900°C and measuring the resulting increase in pressure, using a system in frequent use to determine the hydrogen content of zirconium over a wide range of hydrogen concentrations. Mass spectrometric measurements confirmed that the evolved gas was deuterium.

Tritium Analysis

The tritium analyses were performed by liquid scintillation counting, after distillation to remove dissolved salts.

Titanium/Deuterium Gas System

Experiments were also performed to attempt to duplicate the results reported recently for a metal/deuterium gas system⁽³⁾. One hundred grams of titanium metal sponge, contained in a stainless steel cylinder, was annealed under vacuum at 600°C for two hours. The titanium was allowed to cool to approximately 350°C and then exposed to deuterium gas at a pressure of two atmospheres. This pressure was maintained until the titanium cooled to 50°C and was then increased to 40 atmospheres. The pressure was maintained at 40 atmospheres for 18 hours and the cylinder was then sealed.

The cylinder was immersed in liquid nitrogen. Neutron counting was started within two minutes using detector 5 and continued for 19 hours while the cylinder was maintained at liquid nitrogen temperature. The accumulated counts were recorded every 30 minutes. The deuterium gas pressure was then quickly reduced to atmospheric pressure. After an hour, the remaining deuterium was pumped out, to a pressure of 10^{-3} atmosphere, and the system was gradually warmed to room temperature over a period of 21 hours.

In a second experiment, the pressure and temperature were changed more rapidly. The cylinder containing titanium sponge was pressurized to 40 atmospheres using deuterium gas. This pressure was maintained while the temperature of the cylinder was lowered to that of liquid nitrogen. It was maintained at that temperature for 24 hours. The pressure was then released, the cylinder was pumped down to a pressure of 10^{-3} atmosphere and the temperature gradually increased to room temperature. Neutron counting started immediately using detector 5 and continued for 30 hours, the accumulated counts being recorded every 30 minutes.

RESULTS

Neutron detection

No neutron emission above background was observed for any of the electrolytic cells with any of the neutron detectors. No γ -ray emission above background was observed for cell 1. Neutron detector CRNL 3 has been the most extensively used. Figure 4 shows typical results obtained over a period of a fifteen days with cells 4 and 5 in that detector. A low, constant, signal of $(8.3 \pm 0.6) \times 10^{-3} \text{ s}^{-1}$ is observed. That is not significantly different from the background measured with an unpowered cell in the detector. Table IV summarizes the upper limits of neutron emission and fusion rate observed with the various cells and neutron detectors. The upper limits of neutron emission were calculated for a counting interval of one hour assuming that for a signal to be detectable, the observed signal minus background value has to be at least three times the standard deviation of that observed signal minus background value (99.7% confidence limit). The upper limits for fusion rate were calculated using an arbitrarily selected deuterium to palladium atom ratio of 0.7 and assuming that fusion occurs exclusively through reactions [1] and [2].

Calorimetry

No unexpected heat effects were observed during electrolysis with cells that were equipped with crude temperature measurement systems (cells 3-5, 10 and 11). No excess power could be observed either when cells were electrolysed in the more sensitive and accurate heat-flow calorimeter. This puts an upper limit of 200 mW on the excess power, which corresponds to a maximum specific excess power of 0.13 W.cm^{-3} for the cells used in the heat-flow calorimeter.

Deuterium Loading

The deuterium content of parts of the palladium wire cathode used in cells 1, and 2 was measured after 25 days of nearly continuous electrolysis, using thermal desorption. A deuterium/palladium ratio of 0.72 was obtained for three different samples, indicating that the electrodes had been charged to the palladium hydride β -phase⁽¹²⁾. This represents a lower limit since some deuterium may have been lost during the transfer of the palladium sample from the electrochemical cell to the thermal desorption unit. Hydrogen/palladium ratios of close to 0.9 have been reported for thin foils (0.001x0.2x5 cm) electrolysed in acid solutions for 30 minutes at a current density of 100 mA.cm⁻² ⁽¹³⁾; most of the hydrogen was released from the cathode within 10 seconds of the current interruption.

Tritium Analyses

The tritium content of the solutions were measured both before and after electrolysis for some of the cells (cells 2, 4, 5, 8-10) and for the cells used in the calorimeter. Corrections were made for evaporative losses of D₂O for the cells that did not have a catalytic recombiner. No excess tritium was present after electrolysis in these cells.

Titanium/Deuterium Gas System

No neutron emission above background was observed in the experiments performed with the titanium/deuterium gas system. The upper limits for neutron emission and fusion rate are given in Table IV. The fusion rate was calculated using a deuterium to titanium atom ratio of 2.0 and assuming that fusion occurs exclusively through reactions [1] and [2].

DISCUSSION

Fleischmann *et al.*⁽¹⁾ report a neutron emission of $4 \times 10^4 \text{ s}^{-1}$, measured with a Bonner-sphere type instrument following the electrolysis of 0.1 mol.dm^{-3} LiOD/(99.5% D_2O +0.5% H_2O) at a $0.4 \times 10\text{-cm}$ palladium rod cathode, using a current density of 64 mA.cm^{-2} . They also observed the production of excess power during electrolysis. The specific excess power ranged from 0.095 to 2.7 W.cm^{-3} depending on electrode size, electrode geometry and current density. A total excess energy output of 4 MJ.cm^{-3} over 120 hours is claimed. It should be noted that if the excess power resulted from reactions [1] and [2], then the corresponding neutron emission should be of the order of 10^{13} s^{-1} , a factor 10^9 higher than that measured. No mention is made of the electrolysis time required before excess heat and neutron emission occur. Tritium was detected to the extent of about 1.7 Bq.cm^{-3} in the electrolyte of cells containing $0.1 \times 10\text{-cm}$ palladium rods after electrolysis at 55 mA.cm^{-2} . No mention is made of the initial tritium content of the D_2O . Fleischmann *et al.*⁽¹⁾ also report the emission of 2.2-MeV γ -rays during electrolysis at a $0.8 \times 10\text{-cm}$ palladium rod, which they attribute to reaction [4]. This was, however, subsequently questioned⁽¹⁴⁻¹⁶⁾.

Grundler *et al.*⁽²⁾ report a neutron emission of 36 s^{-1} measured with a similar instrument following the electrolysis of 3 mol.dm^{-3} LiOD/ D_2O at a $1.66 \times 0.7\text{-cm}$ palladium rod. The neutron emission lasted for about 60 hours and is reported to have occurred after a total of about 120 hours of electrolysis at current densities increasing in steps from 40 to 570 mA.cm^{-2} . Excess power was detected simultaneously with the neutron emission. The specific excess power ranged from 0.64 to 2.29 W.cm^{-3} yielding a total excess energy output of about 0.8 MJ over 120 hours. Again, if reactions [1] and [2] are the dominant ones, the excess power is much higher than expected from the reported neutron emission.

Jones *et al.*⁽³⁾ report a neutron emission of the order of 0.06 to 0.4 s^{-1} at 2.5 MeV , measured with a liquid-scintillation neutron spectrometer. This was

obtained during the electrolysis of heavy water containing an acid mixture of salts at titanium or palladium cathodes. The neutron emission is reported to occur after approximately one hour of electrolysis time and to last for about eight hours. From their data, we estimate that a current density of less than $150 \text{ mA}\cdot\text{cm}^{-2}$ was used. No measurement of excess power was performed.

De Ninno *et al.*⁽⁴⁾ report the emission of bursts of neutrons at an average rate of about 10^3 s^{-1} , measured with a $^{10}\text{BF}_3$ detector. This was observed following temperature and pressure cycling of a cylinder containing 100 grams of titanium shavings and deuterium gas. The neutron emissions lasted from 15 to 40 hours.

The above results are summarized in Table IV. We believe that the experimental conditions for our electrolyses are close to those reported in references (1) and (2). Fleischmann *et al.*⁽¹⁾ mention that the excess power observed during electrolysis is a bulk effect and depends on the current density, among other parameters. Figure 5 is a plot of the excess power reported by Fleischmann *et al.*⁽¹⁾, against the product of the mass of the palladium cathode times current density as used in their experiments. The conditions corresponding to their neutron emission and tritium accumulation are also indicated. The arrows on the upper part of the plot show the combinations of palladium mass and current density used in our experiments. It can be seen that as far as these two parameters are concerned, our experimental conditions overlap with those used in reference (1). Our neutron detection efficiency is higher by a factor 10^4 and our background is lower by a factor 10^6 . Our neutron detection efficiency is also higher than in reference (2) by a factor five and our background is lower by a factor 10^3 . Our calorimetric system was sensitive enough to detect the excess specific power reported in (1) and (2). The experimental sections of references (1) and (2) are, however, quite brief and it is possible that important details have been inadvertently omitted. As an example, no accurate mention of electrolysis time is made in reference (1) except for a statement that some experiments were run in excess of 120 hours.

Jones et al.⁽³⁾ describe their experiments in somewhat more detail. As can be seen from Table IV, our neutron detection efficiency and background are such that we would not detect their reported neutron emission. Moreover, their experimental conditions were significantly different from ours (acid solutions, presence of transition metal ions and use of multiple cells in the neutron detector). We cannot thus comment further on their results.

The experimental conditions used for our study of the titanium/deuterium gas system are close to those reported in reference (4). Our neutron detection efficiency is higher by a factor 10^3 and our background is lower by a factor 10^3 .

CONCLUSION

We have used sensitive neutron detectors with low constant backgrounds to measure the neutron emission during electrolysis of heavy water containing $0.1 \text{ mol.dm}^{-3} \text{ LiOH}$, $0.1 \text{ mol.dm}^{-3} \text{ LiOD}$ or $0.5 \text{ mol.dm}^{-3} \text{ D}_3\text{PO}_4$. A variety of electrochemical cells having palladium cathodes in the form of wires, tubes, sheets and rods have been used. The surface area, volume, chemical purity and surface preparation of the cathodes have been varied. We have also used a sensitive and accurate heat-flow calorimeter to measure the energy balance during electrolysis with some of the cells. No neutron emission above background was observed for any of the electrolytic cells with any of the neutron detectors. No excess power could be observed in the calorimetric experiments.

Either the previously reported observations of nuclear and heat effects during the long-term electrolysis of heavy water at palladium electrodes^(1,2) and in the titanium/deuterium gas system⁽⁴⁾ are artifacts, or else our conditions are sufficiently different from those used in references (1,2,4) that similar effects do not occur in

our experiments. The much smaller neutron emission reported by Jones et al.⁽³⁾ is below the detection limit of our neutron detectors.

It is possible that the reported nuclear and heat effects in electrolytic cells depend on on subtle surface, chemical or metallurgical properties of the palladium cathode or on electrochemical parameters such as higher current densities or longer electrolysis times. Similar comments can be made for the titanium/deuterium gas system. More experimentation and time will tell.

ACKNOWLEDGEMENT

We thank Drs. D.P. Jackson, J.S. Geiger, A.I. Miller and G.F. Taylor for support and encouragement.

New Energy Times Archive

REFERENCES

1. M. Fleischmann, S. Pons and M. Hawkins, "Electrochemically Induced Nuclear Fusion of Deuterium", J. Electroanal. Chem. **261**, 301 (1989).
2. W. Grundler, CH. Jung, L. Muller, H.-J. Heidrich, A. Herbst and K.-H. Heckner, "Evidence of Nuclear Fusion Processes in Lithium Containing Palladium Electrodes", Phys. Stat. Sol. (a), in press (1989).
3. S.E. Jones, E.P. Palmer, J.B. Czirr, D.L. Decker, G.L. Jensen, J.M. Thorne, S.F. Taylor and J. Rafelski, "Observation of Cold Nuclear Fusion in Condensed Matter", Nature **338**, 737 (1989).
4. A. de Ninno, A. Frattolillo, G. Lollobattists, L. Martinis, M. Martone, L. Mori, S. Podda and F. Scaramizzi, "Evidence of Emission of Neutrons from a Titanium-Deuterium System", Europhys. Lett., in press (1989).
5. D.V. Balin, E.M. Maev, V.I. Medvedev, G.G. Semenchuk, Yu.V. Smirenin, A.A. Vorobyov, An.A. Vorobyov and Yu.K. Zalite, "Experimental Investigation of the Muon Catalyzed dd-Fusion", Phys. Lett. **141B**, 173 (1984).
6. C.A. Barnes, K.H. Chang, T.R. Donoghue and C. Rolfs, "The $^2\text{H}(d,\gamma)^4\text{He}$ Reaction at Low Energy and the D-State Admixture in ^4He ", Phys. Lett. B, **197**, 315 (1987).
7. H.S. Picker, "On the Fusion of Hydrogen Isotopes in Ordinary Molecules", Nukelonika **25**, 1491 (1980).
8. J.S. Cohen and J.D. Davies, "The Cold Fusion Family", Nature, **338**, 705 (1989).

9. S.E. Koonin and M. Nauenberg, "Calculated Fusion Rates in Isotopic Hydrogen Molecules", *Nature* 339, 690 (1989).
10. S.E. Jones, "Muon-catalysed Fusion Revisited", *Nature* 321, 127 (1986).
11. A.I. Miller, "Deuterium Pilots New Hydrogen Technology", *Int. J. Hydrogen Technol.* 9, 73 (1984).
12. F.A. Lewis, The Palladium Hydrogen System, Academic Press, London (1967).
13. T. Maoka and M. Enyo, "Hydrogen Absorption by Palladium Electrode Polarized in Sulfuric Acid Solution Containing Surface Active Substances - I. The Cathodic Region", *Electrochem. Acta* 26, 607 (1981).
14. R.D. Petrasso, X. Chen, K.W. Wenzel, R.R. Parker, C.K. Li and C. Fiore, "Problems with the γ -Ray Spectrum in the Fleischmann et al. Experiments", *Nature* 339, 183 (1989); and erratum, 339, 264 (1989).
15. M. Fleischmann, S. Pons and R.J. Hoffman, "Measurement of γ -Rays from Cold Fusion", *Nature* 339, 667 (1989).
16. R.D. Petrasso, X. Chen, K.W. Wenzel, R.R. Parker, C.K. Li and C. Fiore, "Measurement of γ -Rays from Cold Fusion - Reply", *Nature* 339, 667 (1989).

FIGURE CAPTION

- Figure 1. Schematic view of a typical electrolytic cell.
- Figure 2. Schematic view of the neutron detection system CRNL 3.
- Figure 3. Counts.hr⁻¹ observed with detector CRNL 3 during the electrolysis of 0.1 mol.dm⁻³ LiOH/D₂O in cells 4 and 5.
- Figure 4. Schematic view of the heat-flow calorimeter: a) cooling water and cover gas system, b) calorimeter and c) electrolytic cell.
- Figure 5. Plot of excess power against the product of the palladium cathode mass times the current density. The dark circles are data from (1). The vertical dashed lines represent the conditions where neutron emission and tritium accumulation have been reported⁽¹⁾. The arrows in the upper part represent the combinations of palladium mass and current density used in our experiments.

Table I. Summary of electrochemical parameters for the electrolytic cells.

CELL	GEOMETRY	DIMENSIONS (cm)	SURFACE AREA (cm ²)	MASS (grams)	CURRENT DENSITY (mA.cm ⁻²)	TIME (days)
Fleischmann <u>et al.</u> ⁽¹⁾	sheet	0.2x8x8	134.	154.	0.8 to 1.6	?
	cube	1x1x1	6.	12.	125 to 250	?
	rods	0.1x10	3.	1.	8 to 512	?
		0.2x10	6.3	4.	" " "	?
		0.4x10	12.6	15.	" " "	?
		0.4x1.25	1.6	2.	" " "	?
Grundler <u>et al.</u> ⁽²⁾	rod	0.7x1.6	3.5	2.	40 to 570	7.5
Jones <u>et al.</u> ⁽³⁾ (4-8 cells)	pellet (Ti)	?	?	1.	?	1 h
	foil	0.0025-thick	3.4	0.05	3 to 150?	?
	sponge	?	?	5.	?	?
This work	wire	0.025x700	19.	4.	20 to 70	7
	wire	"	17.	4.	80 to 200	30
	sheet	0.1x1x9	12.	11.	80	7
	rod	0.7x9	20.	41.	80	10
	rod	0.3x12.5	12.	11.	106	5

Table I. (Continued)

CELL	GEOMETRY	DIMENSIONS (cm)	SURFACE AREA (cm ²)	MASS (grams)	CURRENT DENSITY (mA.cm ⁻²)	TIME (days)
4	rod	0.3x6	5.6	5.	100 to 170	26
5	rod	0.3x10	9.5	8.5	53 to 180	45
6	tubes	0.3x25x0.013	140.	10.5	70 to 100	28
7	tube		3.	2.	100	1
8	tube	0.3x4.4x0.025	8.	1.4	80 to 90	0.5
9	tube	3.3x4.8x0.25	100.	15.	64	0.5
10	tube	3.3x4.8x0.25	100.	15.	64	0.5
11	rod	0.6x5	9.4	17.	100	3

Table II. Summary of chemical parameters for the electrolytic cells

CELL	GEOMETRY	ELECTROLYTE	VOLUME (cm ³)	CHEM. ANAL.	TEMP. (°C)	SURFACE PREPARATION
Fleischmann <u>et al.</u> ⁽¹⁾	sheet	0.1 M LiOH	?	?	?	?
	cube	0.1 M LiOH	?	?	?	?
	rods	0.1 M LiOH	?	?	?	?
Grundler <u>et al.</u> ⁽²⁾	rod	3.0 M LiOD	60	?	25	electron-beam melted, cold-worked
Jones <u>et al.</u> ⁽³⁾	pellet (Ti)	salts	20	?	?	dilute acid
	foil	+	20	?	?	& abraded
	sponge	10 ⁻³ M HNO ₃	20	?	?	(sometimes)
This work						
	1	wire	0.1 M LiOH	99.95%	20	none
	2	wire	0.1 M LiOH	99.95%	16	none
	2	sheet	0.1 M LiOH	0.13 at.% Ag	16	none
				Atomic absorption		
	2	rod	0.1 M LiOH	0.13 at.% Ag	16	arc-melted, cast, swaged, annealed, cleaned with acetone, aqua regia and water, abraded (600 grit)

Table II. (Continued)

CELL	GEOMETRY	ELECTROLYTE	VOLUME (cm ³)	CHEM. ANAL.	TEMP. (°C)	SURFACE PREPARATION
3	rod	0.1 M LiOH	350	10 ppm Ag	16	arc-melted, cast,
				DC arc, XPS		swaged, annealed,
						electropolished,
						washed with methanol
4	rod	0.1 M LiOH	45	"	16	"
5	rod	0.1 M LiOD/D ₂	55	99.95%	16	washed with alcohol
6	tubes	0.1 M LiOH	150	3 at.% Ag	--	none
7	tube	0.1 M LiOH	--	100 ppm Ag	--	none
				Neutron Activat.		
8	tube	0.5 M D ₃ PO ₄	5	none	--	none
9	tube	0.5 M D ₃ PO ₄	250	none	--	none
10	tube	0.1 M LiOD	250	none	50	none
11	rod	0.1 M LiOD	250	99.95%	20	none

Table III. Summary of important parameters for the neutron detectors

	SHIELD	MODERATOR	DETECTOR	EFFICIENCY (%)	BACKGROUND* (10^{-3} s^{-1})
CRNL 1	wax	wax	1 ^3He	~ 0.1	4.2 ± 1
CRNL 2	wax, cadmium	wax	3 ^3He	~ 0.7	2.5 ± 0.8
CRNL 3	wax, cadmium	wax	5 ^3He	1.6 ± 0.8	8.3 ± 1.5
				(Pu/Be, Pu/Li, ^{252}Cf)	
CRNL 4	wax, water, concrete	wax	1 $^{10}\text{BF}_3$	1.0	2.20 ± 0.08
				(Pu/Be)	
WNRE 1	polyethylene, cadmium	polyethylene	8 ^3He	~ 1.5	73 ± 4
WNRE 2	cadmium, concrete, polypropylene	polypropylene	6 ^3He	~ 1.5	13.5 ± 0.4

* for a one hour counting period

Table IV. Neutron detection summary

CELL	DETECTOR	TIME IN DETECTOR (days)	NEUTRON FLUX (s ⁻¹)	FUSION RATE ^a TiD ₂ , PdD _{0.7} (fus.s ⁻¹ per D-D)
Fleischmann et al. ⁽¹⁾	Bonner-sphere	2	4x10 ⁴ , (2 d) ^b	3x10 ⁻¹⁸
Grundler et al. ⁽²⁾	Bonner-sphere	2	36, (2 d) ^b	8x10 ⁻²²
Jones et al. ⁽³⁾	Scintillator	0.3 ?	0.06 to 0.4, (1-8 h) ^b	(0.15-1)x10 ⁻²³
De Ninno et al. ⁽⁴⁾	¹⁰ BF ₃	2	(0.4-5)x10 ³ , (10 min) ^b	(0.3-4)x10 ⁻²¹
This work				
Ti/D ₂ (g) 1 2 3 4 5 6 7 8 9 10 11	CRNL 4	1	<0.5, (1 h, 3σ) ^b	<4x10 ⁻²⁵
	CRNL 1	7	<6.	<7x10 ⁻²³
	CRNL 2	7	<0.7	<6x10 ⁻²⁴
	CRNL 3	5	<0.5	<2x10 ⁻²³
	CRNL 3	9	<0.5	<5x10 ⁻²³
	CRNL 3	16	<0.5	<3x10 ⁻²³
	CRNL 2	1	<0.7	<3x10 ⁻²³
	CRNL 4	1	<0.5	<10 ⁻²²
	WNRE 1	0.5	<1.4	<5x10 ⁻²²
	WNRE 2	0.5	<1.7	<10 ⁻²²
	WNRE 2	0.5	<1.7	<10 ⁻²²
	WNRE 2	3	<1.4	<4x10 ⁻²³

a) calculated assuming that fusion occurs exclusively through reactions [1] and [2]; b) counting interval.

F1A-2

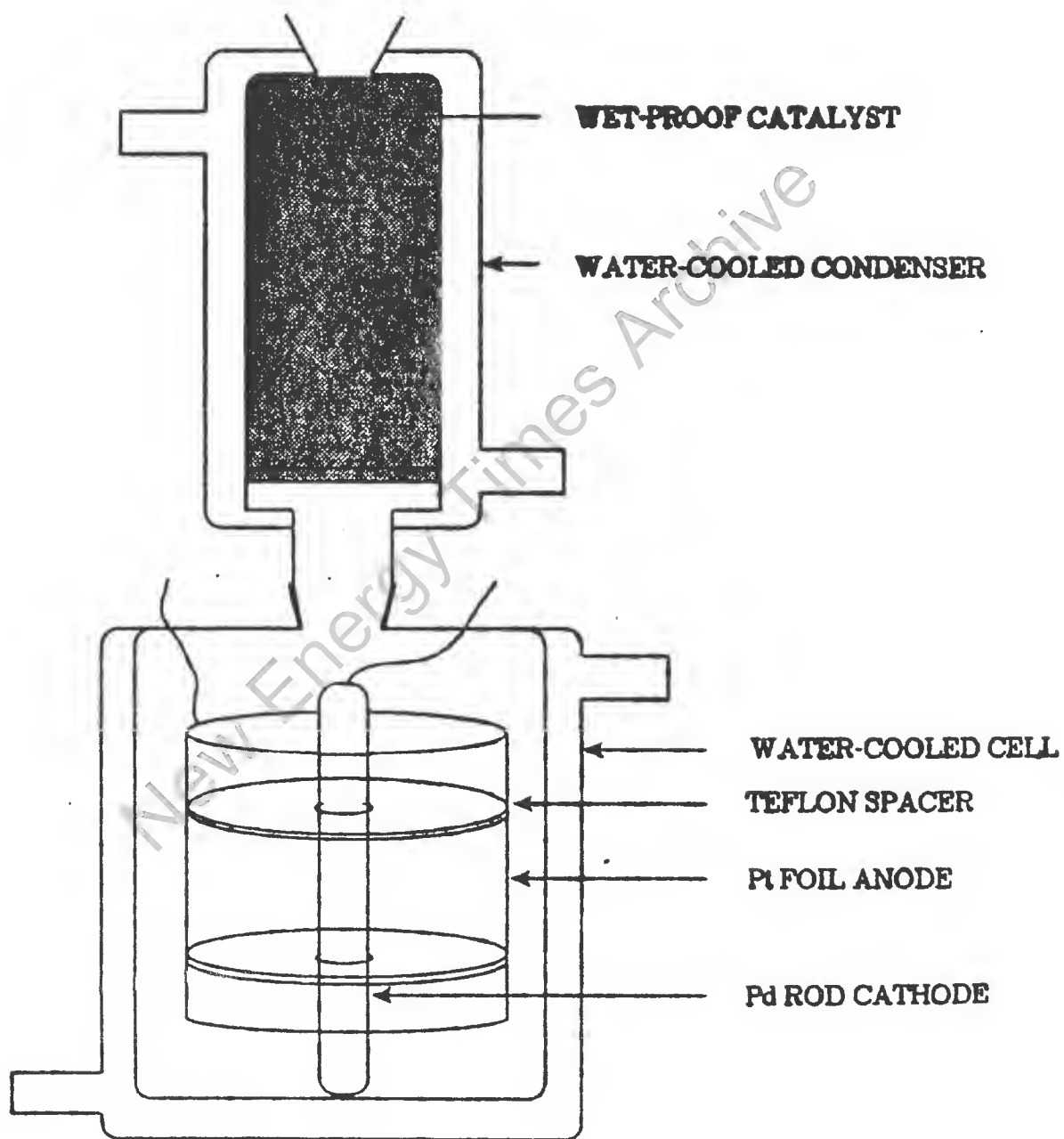
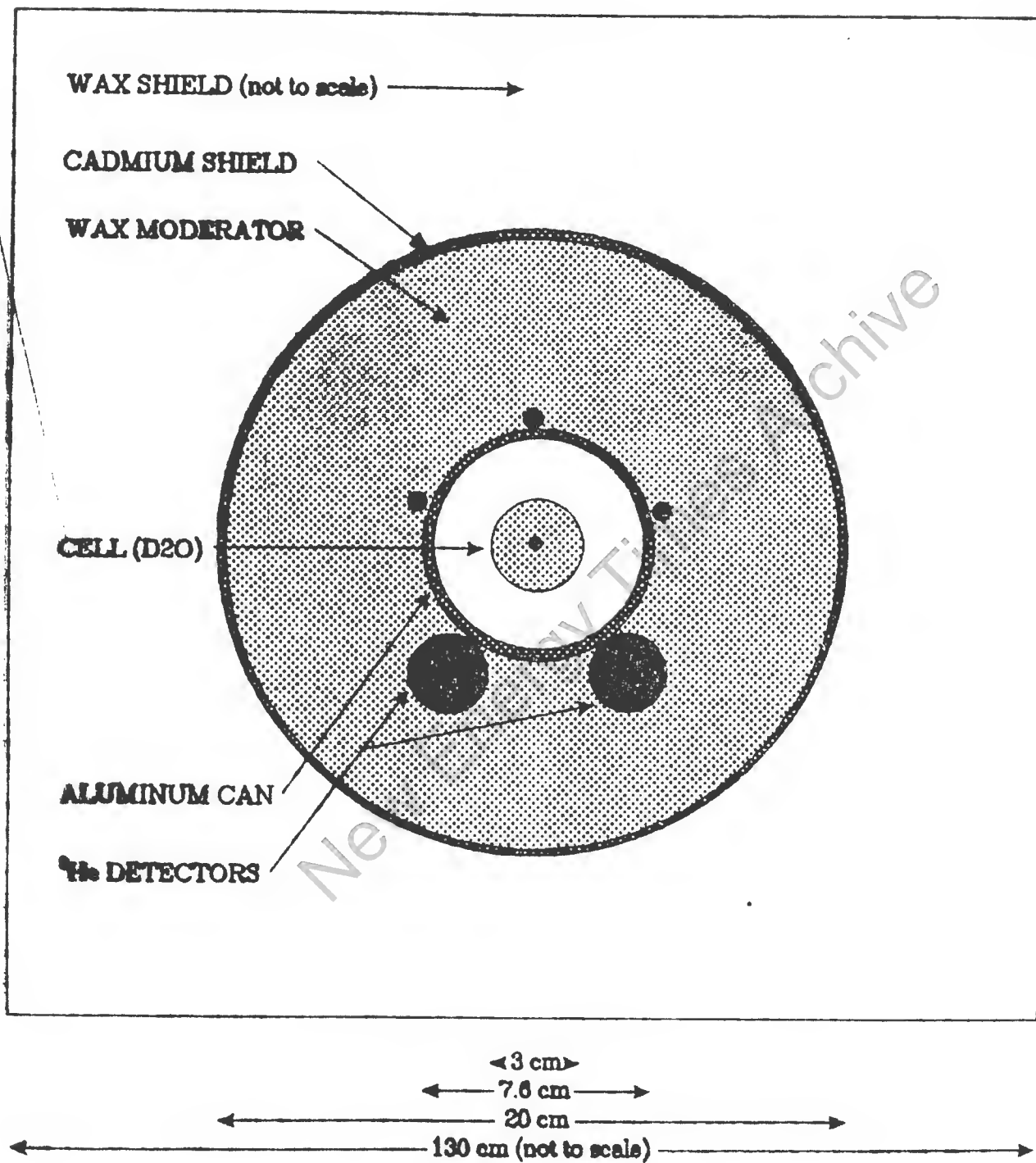


Fig. 6.



DETECTOR CRNL3, CELLS 4 & 5

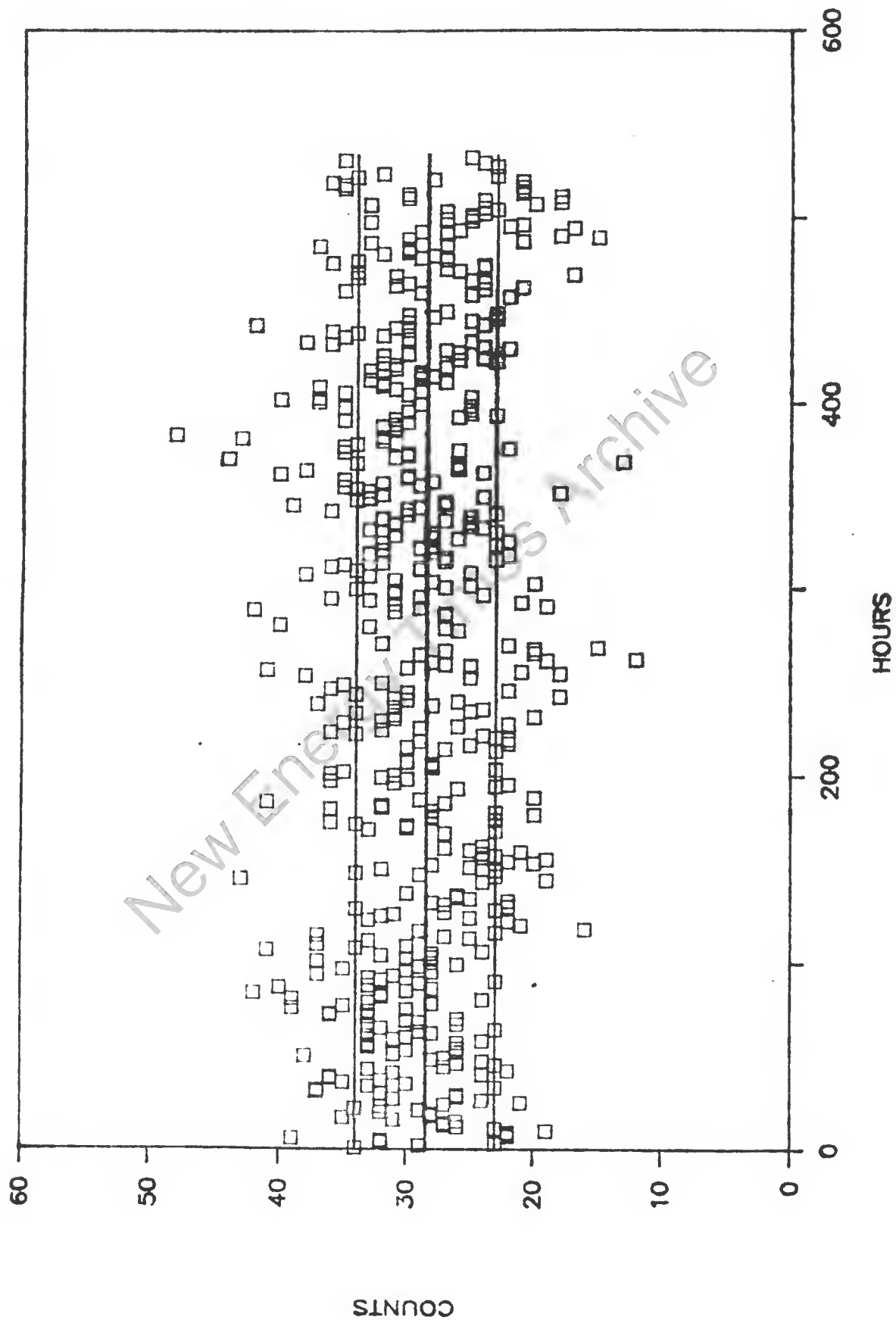
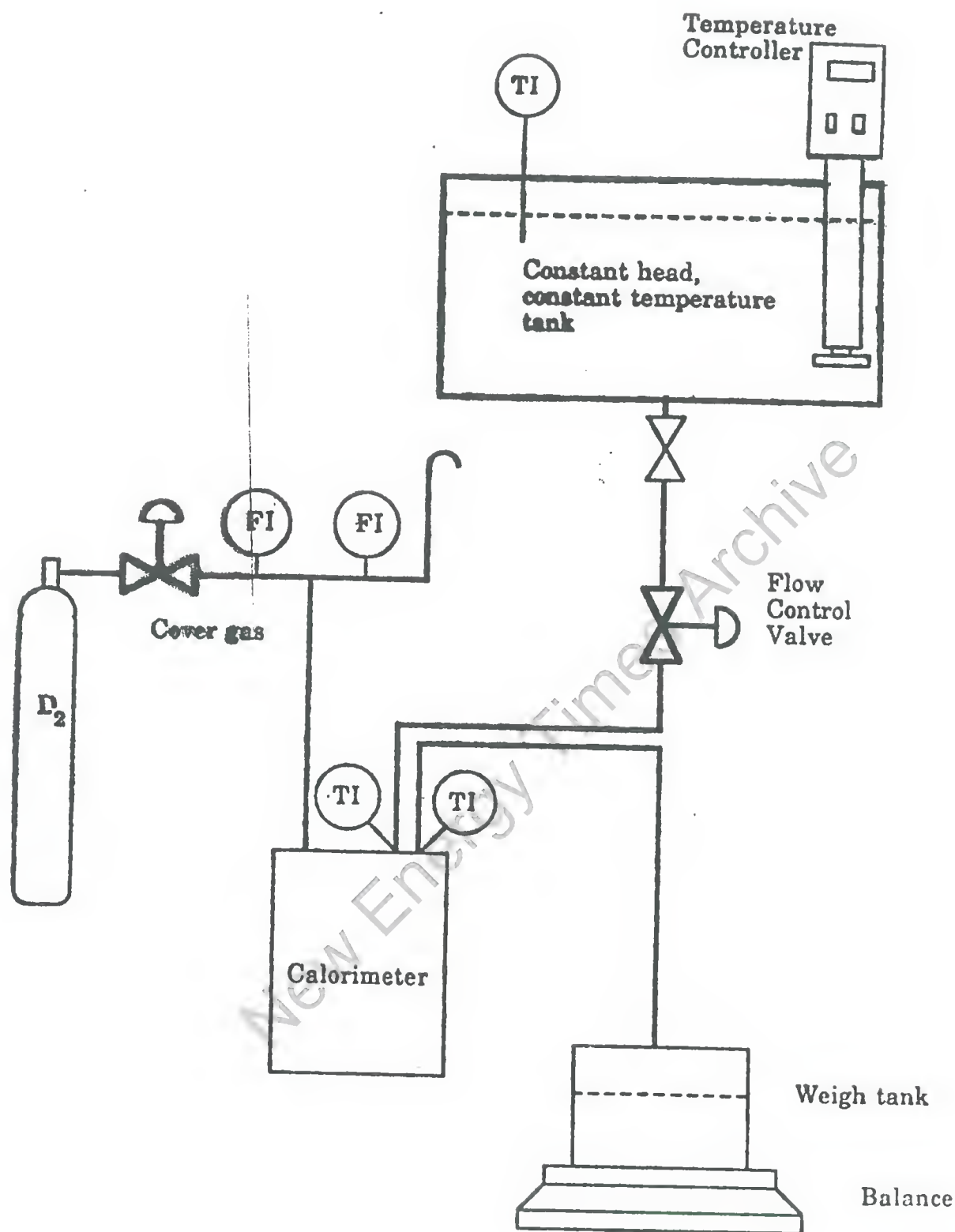


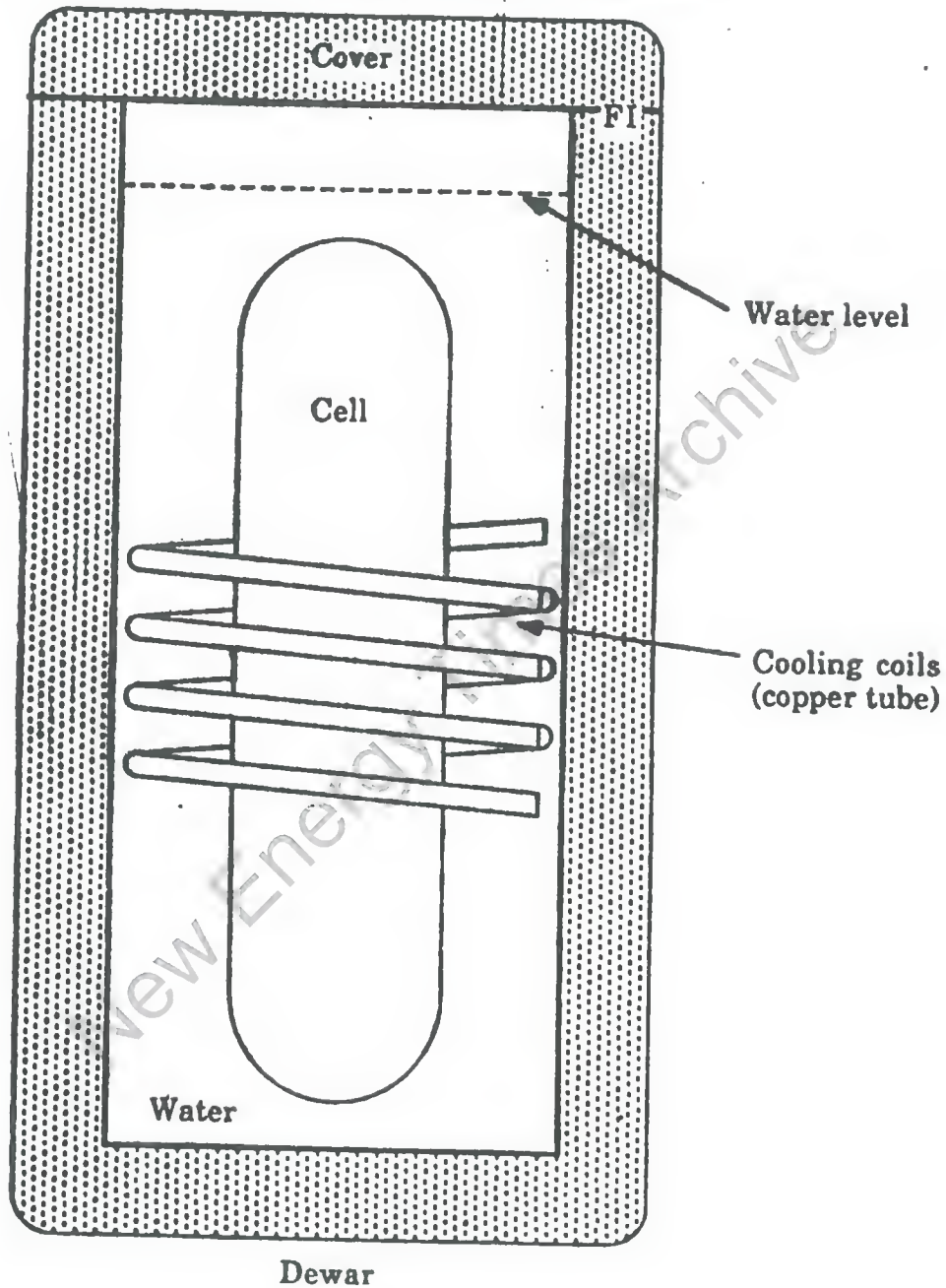
Fig. 1.1



Cooling water and cover gas system

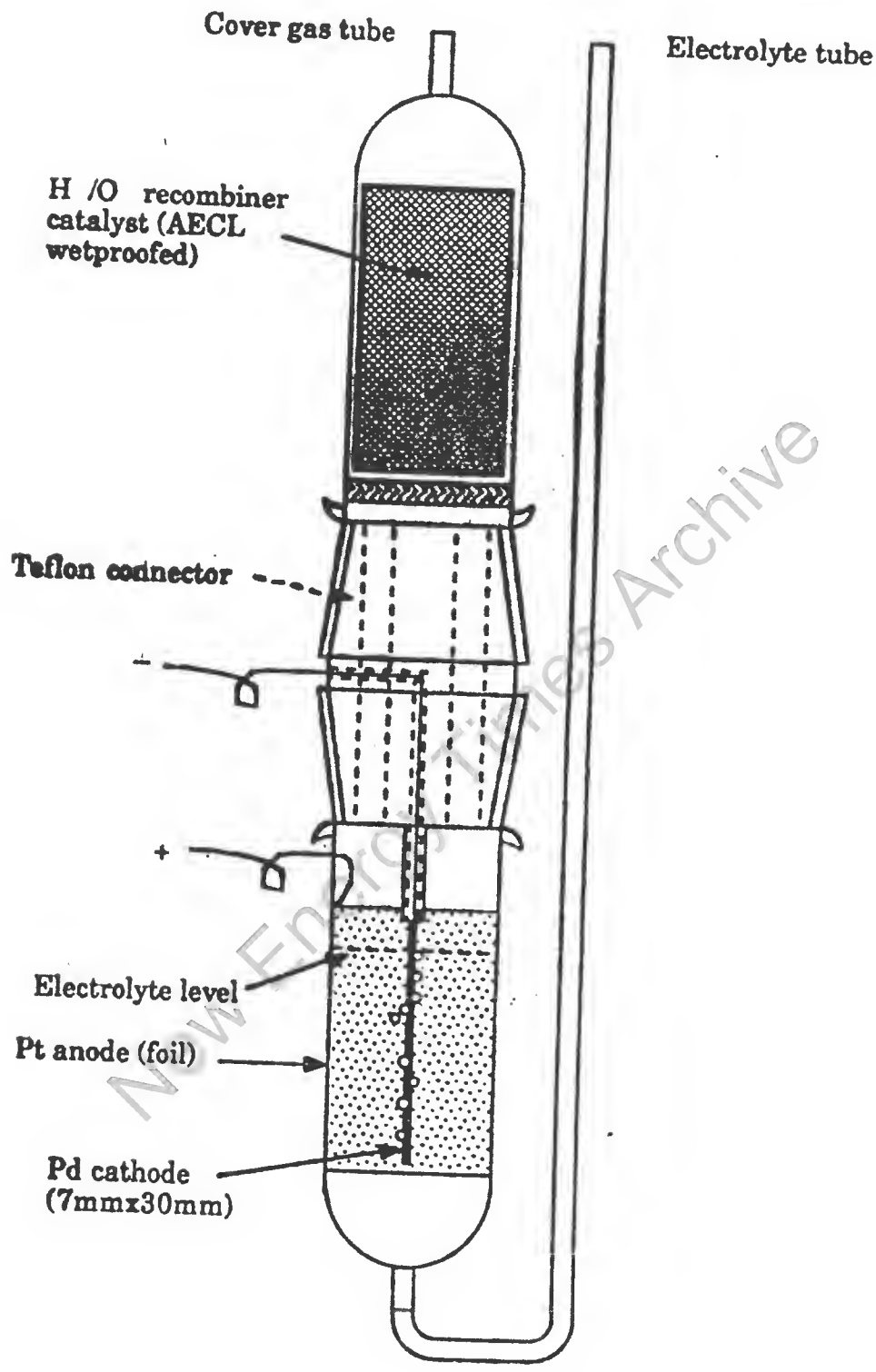
FL-411

Connections made through the cover:
Electrical, cooling water, electrolyte, cover gas



Flow Calorimeter (schematic)

FIG. 4c)



Cell (glass)

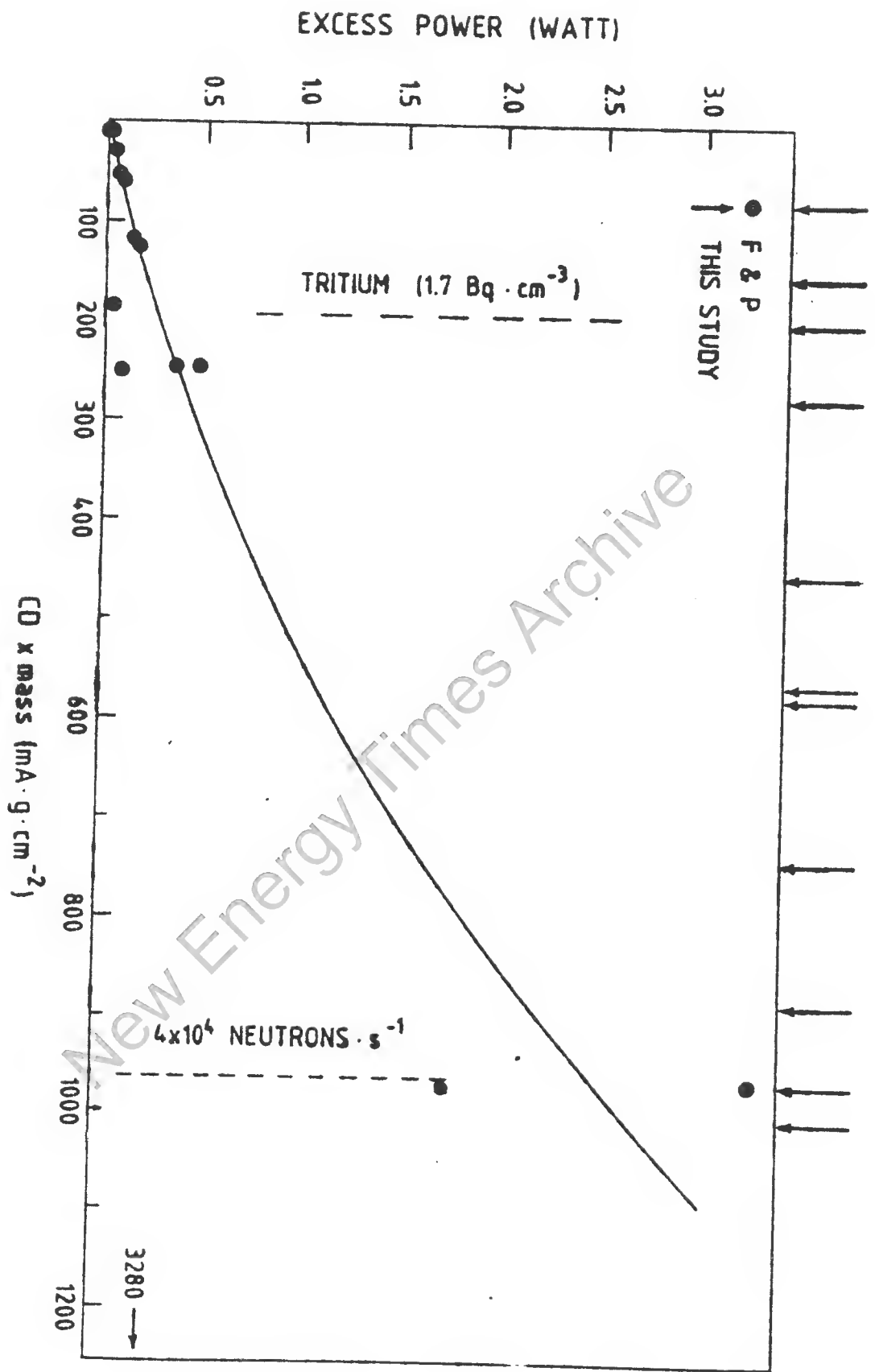


FIG. 5